RSC Advances

PAPER

View Article Online
View Journal | View Issue

Cite this: *RSC Adv.*, 2014, **4**, 8828

Design and synthesis of ERα/ERβ selective coumarin and chromene derivatives as potential anti-breast cancer and anti-osteoporotic agents†

M. Kamil Hussain,[a] M. Imran Ansari,[a] N. Yadav,[a] Puneet K. Gupta,[a] A. K. Gupta,[a] R. Saxena,[b] I. Fatima,[b] M. Manohar,[b] P. Kushwaha,[b] V. Khedgikar,[b] J. Gautam,[b] Ruchir Kant,[c] P. R. Maulik,[c] R. Trivedi,[b] A. Dwivedi,[b] K. Ravi Kumar,[d] A. K. Saxena[a] and K. Hajela*[a]

Received 11th October 2013
Accepted 25th November 2013

DOI: 10.1039/c3ra45749d

www.rsc.org/advances

Several new coumarin and chromene prototype derivatives have been synthesised and evaluated for their ERα and ERβ selective activity. Coumarin prototype compounds **18** & **19** were found to be ERα selective and the most active, exhibiting potential antiproliferative activity against both ER +ve & ER −ve breast cancer cell lines. The surprise finding of the series, however, are the novel prototype III chromenes **45** & **46**, with aroyl substitution at the 6th position. Both the compounds have shown potent antiproliferative activity against both the breast cancer cell lines, promote alkaline phosphatase activity, enhance osteoblast mineralization *in vitro*, significantly decrease ERE–ERα dependent transactivation and induce ERβ activity. This specific upregulation of ERβ isoform activity of compound **45** may be responsible for the antiosteoporotic activity at picomolar concentration. In addition, both the compounds were also devoid of any estrogenic activity, which correlates to their antiestrogenic behaviour in the two breast cancer cell lines. Assessment of selectivity using specific SiRNAs for ERα and ERβ revealed that most of the compounds showed ERα and ERβ-mediated action, except compound **28**, which showed selectivity to ERα only. Computational docking analysis of active compounds **18** and **45** was conducted to correlate the interaction with the two receptors and it was found that the docked conformations of the coumarin prototype, compound **18** at ERα and ERβ active sites were more or less superimposable on each other. However, the unique orientation of the aminoalkoxy side chain of novel chromene (prototype III) compound **45** in the ERβ binding cavity may be responsible for its potential biological response.

1. Introduction

Mammary carcinoma is the most common malignancy in women and the leading cause of cancer death among females, accounting for 23% of the total cancer cases and 14% of all cancer deaths. An estimated 1.7 million women will be diagnosed with breast cancer in 2020, which is a 26% increase from current levels.[1,2] The steroid hormone estrogen mediates a number of biological processes, ranging from reproductive health to bone maintenance, through estrogen receptors (ER), a member of a large superfamily of nuclear receptors (NR).[3] The same estrogen is also predominantly involved in the initiation and proliferation of ER +ve breast cancer and much effort is now being devoted to block estrogen formation and action. The ER exists in two isoforms, α (ERα) and β (ERβ), both of which are ligand-induced transcription factors that have different distributions in various estrogen target tissues and also have different functions, some of which have not yet been clarified. ERα and ERβ share modest overall sequence identity (47%), where the DNA and ligand-binding domains are highly conserved with only minor structural differences, but there is little or no detectable homology between their N-terminal transactivation (AF-1) domains.[4–6] ERα, the predominant subtype expressed in breast cancer, induces proliferation in response to estrogen, while ERβ, the predominant subtype present in bone, colon and prostrate, inhibits proliferation of breast cancer cells by antagonizing the function of ERα and also checks the development of osteoporosis. Thus ERα and ERβ are

[a]*Medicinal and Process Chemistry Division, CSIR-Central Drug Research Institute, Sector 10, Jankipuram Extension, Sitapur Road, Lucknow-226031, India. E-mail: kanchan_hajela @cdri.res.in; Tel: +91-522-261241-18, PABX, 4679/4680*

[b]*Endocrinology Division, CSIR-Central Drug Research Institute, Lucknow-226031, India*

[c]*Molecular and Structural Biology Division, CSIR-Central Drug Research Institute, Lucknow-226031, India*

[d]*X-ray Crystallographic Division, CSIR-Indian Institute of Chemical Technology, Hyderabad-500007, India*

† Electronic supplementary information (ESI) available: X-ray Crystallographic data of compound **18**, spectroscopic data, copies of ^{1}H and ^{13}C NMR spectra of compounds and 2D binding pose view of ligands at the binding site of ER-α and ER-β. CCDC 962314. For ESI and crystallographic data in CIF or other electronic format see DOI: 10.1039/c3ra45749d

potential targets for the treatment of breast and endometrial cancers. Mapping the distribution of ERα and ERβ mRNA in normal and neoplastic tissues has provided an intriguing picture of differential expression patterns in different tissue types. This existence of clear-cut differences in the two subtype receptor expressions suggests that tissues could be differentially targeted with receptor selective ligands.[7–11] The most widely used strategy to disrupt estrogen mediated breast cancer proliferation is through targeted antagonism of estrogen receptors in the breast tissues by antiestrogens or SERMs, a new class of tissue selective therapeutic agents called "designer molecules" with specific interactions in the target cells leading to tissue selective action.[12–15]

Coumarins, a class of naturally occurring benzopyrone derivatives, comprise a vast array of biologically active compounds found in a variety of plant sources. They display interesting pharmacological properties, which have encouraged medicinal chemists for decades to explore the natural coumarins or their synthetic analogues for their applicability as drugs.[16a,b] The coumarins are extremely variable in structure due to the presence of different types of substitutions in their basic structure, which can influence their biological, pharmacological and therapeutic applications.[17,18] Hydroxycoumarins act as potent metal chelators and free radical scavengers and the active metabolite 7-hydroxycoumarin derivatives have shown sulfatase and aromatase inhibitory activities.[19] Coumarin based selective estrogen receptor modulators (SERMs) and coumarin–estrogen conjugates have been described as potential anti-breast cancer agents.[19] Recently, coumarin based new generation SERM, SP500263 is reported to be a highly potent antiestrogen currently under clinical investigation.[20]

With the emergence of drug resistance as a major new impediment in breast cancer treatment, combined with the problems of low tumor selectivity and toxicity, there is an urgent need for the discovery of less toxic and potent new anti-breast cancer drugs, which target the interactive mechanisms involved in growth and metastasis of breast cancer.[21,22] The emerging role of ERβ in hormone related cancers has opened the possibility of developing new ERβ inducing agents. Therefore the search for novel pharmacophores eliciting opposing action on ERα or ERβ may provide a rationale for developing a drug that might have bone protective effects in addition to anti-cancer effects. In this paper, we report the structural design and synthesis of some novel coumarin/chromene based molecules of prototypes **I**, **II** and **III** and their biological efficacy for selective ER mediated anti-breast cancer and anti-osteoporotic activities.

2. Results and discussion

2.1. Chemistry

The synthesis of all the target molecules was achieved through efficient synthetic routes. For the synthesis of prototype molecules **I**, benzils **3** and **5**, which formed the key precursors, were prepared as follows. Sonogashira coupling of 4-iodoanisole with commercially available 2-methoxy phenylacetylene conveniently formed the 2,4′-dimethoxy diphenyl acetylene,[23] **1** which on oxidation with PdI_2 in DMSO gave the corresponding 2,4′-dimethoxybenzil **2** in >90% yields.[24] Subsequent demethylation under basic conditions using ethanethiol–sodium hydride in dry DMF led to the hydroxy derivative **3**. The product was isolated as a yellow solid in 95% yield, mp 162–163 °C.[25a,b] The synthesis of 2,4′-dihydroxy-4-methoxy benzil **5** was carried out by the acylation of 3-methoxyphenol with 4-hydroxy phenylacetic acid, followed by the oxidation of the resulting deoxybenzoin **4** with selenium dioxide in dioxane–water (Scheme 1).[26,27]

For the synthesis of 4-aroylated coumarins, we have developed a simple methodology and report the synthesis of 3-aryl-4-aroyl coumarin, as the desired scaffold, for the first time through condensation of benzils with aryl acetyl chlorides (Scheme 2).

The reaction of benzils **3** and **5** with phenyl or 4-methoxyphenyl acetyl chlorides **6** or **7** under reflux in acetone and anhydrous potassium carbonate afforded coumarins (**8–11**) in pure form by simple crystallisation and without any chromatographic purification in excellent yields (90–95%). Subsequent base catalysed O-alkylation of the hydroxy group of compounds **8–11** with piperidine/pyrrolidine 1-(2-chloroethyl) monohydrochlorides formed the target compounds, 3-phenyl/4-methoxy-phenyl-7-methoxy-4-[-4-(2-piperidinyl/pyrrolidinyl) ethoxy benzoyl]coumarins (**12–19**) in good yields.

Since the presence of hydroxy groups at appropriate positions plays a prominent role in the binding of ligands to the biological target, the estrogen receptors, it was thought worthwhile to demethylate the methoxy derivatives to the corresponding hydroxy compounds. A combination of ethanethiol with anhydrous aluminium chloride in dry DCM at 0–10 °C was used for demethylation of (**8–11** and **12–19**), which conveniently gave the corresponding phenolic analogues (**20–22** and **23–28**) in high yields.

The chemical methodology, which was followed to synthesize compounds of prototype **II**, is shown in Scheme 3. The starting precursor, 7-methoxy isoflavanone **30**, was easily prepared by base catalyzed condensation of 2-hydroxy-4-methoxy deoxybenzoin **29** with paraformaldehyde.[28] The introduction of an aroyl group at the 4-position of the isoflavene by

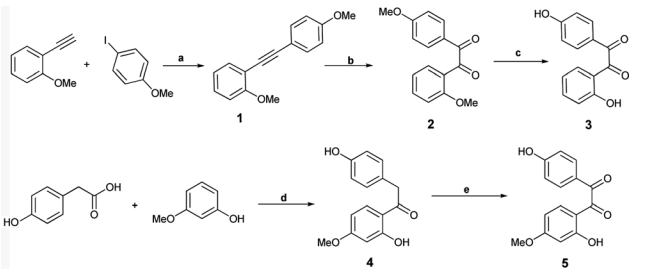

Scheme 1 Synthesis of 2,4′-dihydroxy and 2,4′-dihydroxy-4-methoxy benzils (compounds **3** and **5**). *Reagents and reaction conditions* (a) $Pd(PPh_3)_4Cl_2$, CuI, Et_3N, N_2, RT, 90%. (b) PdI_2, DMSO,140 °C, 95%. (c) EtSH–NaH, DMF, 0 °C–120 °C, 95%. (d) BF_3.OEt, N_2, 85 °C, 90%. (e) SeO_2, 1,4-dioxane/H_2O; (24 : 1), 110 °C, 90%.

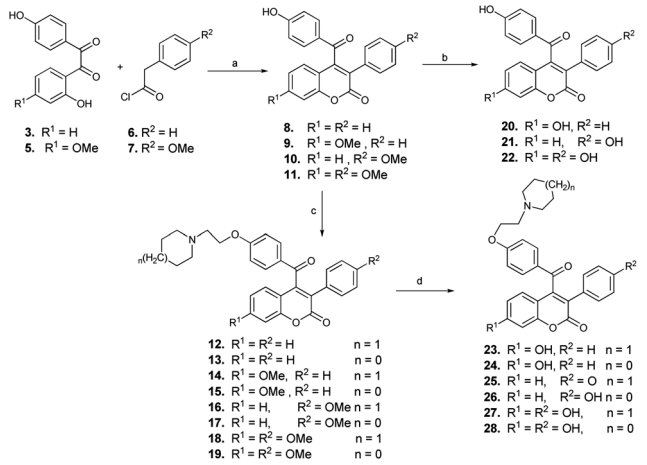

Scheme 2 Synthesis of molecules of prototype I (compounds **8–28**). *Reagents and conditions*: (a) acetone, K_2CO_3, reflux, 4–5 h, 90–95%. (b) EtSH, $AlCl_3$, DCM, 0 °C, 3 h. (c) piperidine/pyrrolidine 1-(2-chloroethyl) monohydrochlorides, acetone, K_2CO_3, reflux, 3–4 h, 90–95%. (d) EtSH, $AlCl_3$, DCM, 0 °C, 3 h, 90%.

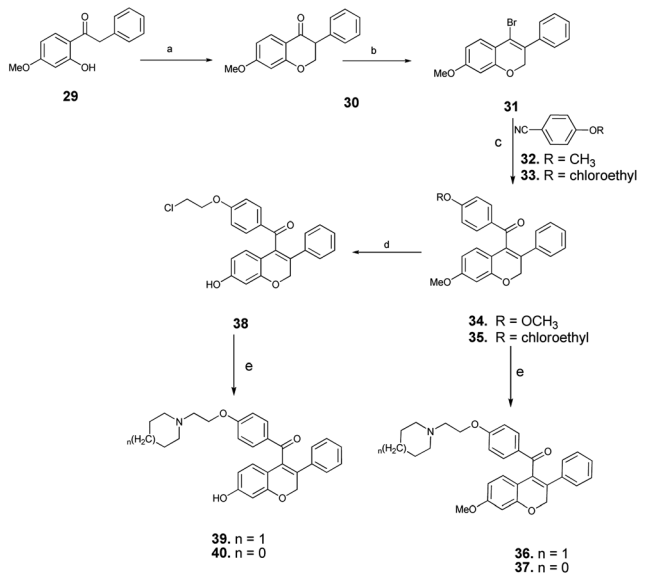

Scheme 3 Synthesis of molecules of prototype II (compounds **34–40**). *Reagents and reaction conditions*: (a) $(HCHO)_2$, 25% aq. Me_2NH, EtOH, reflux,75%, (b) PBr_3, benzene, 80 °C, 85%, (c) 1.6 M *n*-butyllithium in hexane, dry ether, N_2, 0–5 °C, 70–75%, (d) EtSH/$AlCl_3$, DCM, 0 °C, 3 h, 85%, (e) piperidine/pyrrolidine, dry DMF, TBAI 80 °C, 90–95%.

direct aroylation (obtained by reduction and subsequent dehydration of isoflavonone **30**) was not successful. Subsequently, it was thought to introduce the aroyl functionality through formation of 4-bromo isoflavene **31**. Refluxing of the compound **30** with PBr_3 in dry benzene formed the desired 4-bromo isoflavene **31** in excellent yield and was isolated as a white solid on crystallisation from methanol. However, it was found to be unstable (decomposed at rt) and was therefore immediately subjected to anion formation with *n*-butyl lithium at 0 °C, followed by quenching with 4-methoxy benzonitrile or 4-chloroethoxy benzonitrile to afford the 7-methoxy-4-(4-methoxy/chloroethoxy) benzoylated chromenes **34** and **35** in good yields. Subsequent reaction of compound **35** with piperidine or pyrrolidine in the presence of TBAI in dry DMF formed the aminoalkoxy compounds **36** and **37**. Cleavage of the methyl ether linkage of compound **35** using EtSH/anhy. $AlCl_3$ formed the phenolic derivative **38**, which on further reaction with piperidine and pyrrolidine in dry DMF–TBAI gave the target phenolic compounds **39** and **40**.

Having successfully achieved the synthesis of prototype compounds **I** and **II**, we next directed our efforts to synthesise prototype **III** molecules, as shown in Scheme 4. The envisaged precursor, 7-methoxy-3-phenyl-coumarin **41**, was easily prepared in quantitative yields through the condensation of 2,4-dihydroxy benzaldehyde with phenyl acetic acid, followed by subsequent deacetylation of the 7-hydroxy group and finally its methylation. A *gem*-dimethyl group was introduced through Grignard reaction with an excess of freshly prepared methylmagnesium iodide at the 2nd position of **41**, forming 7-methoxy-2,2-dimethy-3-phenyl-2*H*-chromene **42** in good yields.[29] Again, for the introduction of the aroyl group at the 4-position of chromene **42**, the synthetic plan through formation of 4-bromo derivative of isoflavene **42** was not successful.

The next option of direct aroylation of **42** with 4-methoxy benzoyl chloride was carried out using $SnCl_4$ in dry DCM and, surprisingly, the reaction was successful. Spectral analysis of the isolated product by ^{1}H NMR showed three singlets, each integrating for one proton in the aromatic region. This indicated regioselective aroylation, probably occurring at the 6th position of the chromene **42** instead of at the 4th position. The structure was finally confirmed by HMBC spectral analysis. The proton at the C-5 position of the chromene ring showed three bond correlations with signals of the carbon of the carbonyl group as well as the C-7 carbon. On the other hand, the proton at the C-8 position showed a 3-bond correlation with the C-6 carbon signal and the proton at the C-4 position showed a

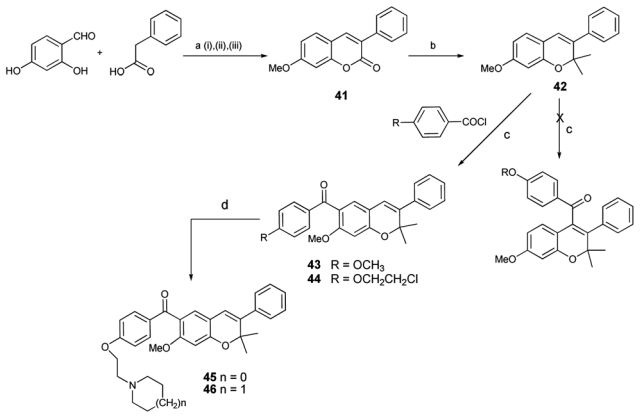

Scheme 4 Synthesis of molecules of prototype III (compounds **43**, **45** and **46**). *Reagents and conditions*: (a) (i) Ac_2O, TEA, reflux, 78%, (ii) MeOH, K_2CO_3 RT, 90%, (iii), K_2CO_3, acetone, MeI, reflux, 92%; (b) MeMgI, THF, reflux, conc. HCl, 70%; (c) $SnCl_4$, DCM, 0 °C, 1 h 95%; (d) piperidine or pyrrolidine, dry DMF, TBAI 80 °C, 6 h, 92%.

3-bond correlation with the C-2 carbon signal. These correlations confirmed the presence of an aroyl group at the 6th position, as shown in Fig. 1. It can be speculated that the presence of the methoxy group at the 7th position may be the driving force for the aroylation at the 6th position being more nucleophilic as compared to the 4th position. The 6-aroylated chromenes **43** and **44** were obtained in pure form by simple crystallization in excellent yield. Reaction of compound **44** with pyrrolidine or piperidine, respectively, in the presence of TBAI in dry DMF at 80 °C, formed the corresponding alkylaminoalkoxy derivatives **45** and **46**, thus completing the synthesis of prototype **III** compounds.

2.2. Biological evaluation

2.2.1. *In vitro* anti-proliferative activity. The biological efficacy of the target compounds was first explored for their antiproliferative activity against a panel four different human tumor cells from breast MCF-7 (ER +ve) and MDA-MB-231 (ER −ve) cell lines, endometrial using Ishikawa cell line and prostrate on the PC-3 cell line using MTT assay and they were compared with reference compounds tamoxifen and raloxifene. All the compounds were also tested for toxicity in normal human kidney cell line HEK-293 and were found to be non-toxic to the normal cells.

Of the first prototype **I**, molecules **8–28**, which had a basic coumarin nucleus substituted with variable 3-aryl and 4-aroyl groups, it was found that in general the compounds displayed anti-proliferative activity against the both ER +ve & ER −ve breast cancer cell lines and an almost negligible activity against the Ishikawa and PC-3 cell lines. Three compounds **9**, **18** & **19**, showed very good activity. Compound **18** was the most active, showing IC_{50} of 5.7 μM in MCF-7 cells, and 12.7 μM in MDA-MB 231 breast cancer cells, better than tamoxifen and raloxifene, used as a positive control, which showed IC_{50} of 13.7 in MCF-7 and 17.9 μM in MDA-MB 231 cells. Similarly, compound **19** also showed comparable inhibition of both breast cancer cell lines. In prototype **II** molecules, where the basic pharmacophore was changed from coumarin to chromene, the activity was considerably decreased in compounds **34**, **36**, **37**, **39** and **40**. Only two compounds, **34** and **36**, showed growth inhibitions in both the cell lines. However, the introduction of a *gem*-dimethyl group at the 2nd position of the chromene pharmacophore, coupled with aroyl functionality at the 6th position instead of at the 4th position in the prototype **III** molecules, resulted in a better activity profile, and all three compounds **43**, **45** and **46** showed substantial growth inhibition against both the breast cancer and Ishikawa cell lines. Compared to tamoxifen, compounds **45** and **46** showed potent inhibition in the range 6.8 μM to 8.1 μM against the MCF-7 cell line. The compounds did not show any significant antiproliferative activity against the prostate cancer cell line and only four compounds **17**, **19**, **23** & **25** were moderately active (Table 1 and Fig. 2a–c).

2.2.2. Relative binding affinity to ER. In order to confirm if the action of active compounds is mediated through ER, their ER binding potential was evaluated using a competitive binding assay, employing radio labeled estradiol (^3H–E_2) as the reference compound. Briefly, the uterine cytosol (obtained from immature 20–21 days old-estradiol primed rats) was incubated with ^3H–estradiol in the absence or presence of various concentrations of test compounds for 22 h at 4 °C. ^3H–E_2 bound and free fractions were separated by a charcoal adsorption method. The relative binding affinity of each test compound was calculated from the graph of percentage bound radioactivity verses molar concentration of the test substance. At 50% inhibition, the log of the competitor concentration relative to that of estradiol expressed the affinity of the test compound to ER relative to estradiol. This, when multiplied with 100, gave the % value designated as RBA (Table 1). The results indicate that

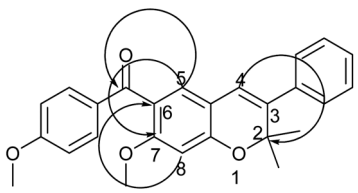

Fig. 1 Significant HMBC (H → C) correlation of compound **43**.

Table 1 *In vitro* anti-proliferative activity and receptor binding affinity of coumarin and chromene derivatives against different cancer cell lines

IC_{50} values (μM)					
Compound no.	MCF-7	MDA-MB 231	Ishikawa	PC-3	% RBA
8	24.3	>40	>40	>40	0.05
9	17.7	34.2	ND	>40	0.02
10	27.9	37.8	ND	>40	0.026
11	>40	>40	ND	>40	0.05
12	>40	>40	>40	>40	3
13	33.7	>40	>40	>40	0.3
14	29.3	>40	ND	>40	0.114
15	32.4	31.2	ND	>40	0.285
16	19.7	20.5	ND	>40	0.8
17	16.3	18.8	ND	22.8	1.3
18	5.7	12.7	>40	>40	0.16
19	12.8	18.4	>40	22.5	0.1
20	22.1	34.3	ND	>40	34
21	>40	>40	ND	>40	0.08
22	>40	>40	ND	>40	6
23	>40	>40	>40	28.6	11.42
24	>40	>40	>40	>40	16
25	31.7	>40	ND	18.8	2
26	>40	>40	ND	>40	2.6
27	25.9	>40	ND	>40	12.3
28	27.1	>40	ND	>40	13.3
34	20.0	>40	ND	>40	0.05
36	34.5	>40	>40	>40	0.3
37	>40	17.5	>40	>40	0.6
39	>40	>40	ND	>40	0.1
40	>40	>40	ND	>40	2.25
43	19.8	20.2	15	ND	0.09
45	6.8	16.9	17.7	>40	0.225
46	8.1	14.8	16.9	>40	0.6
Tamoxifen	13.7	17.9	ND	>40	2.25
Raloxifene	15.4	18.5	ND	>40	15

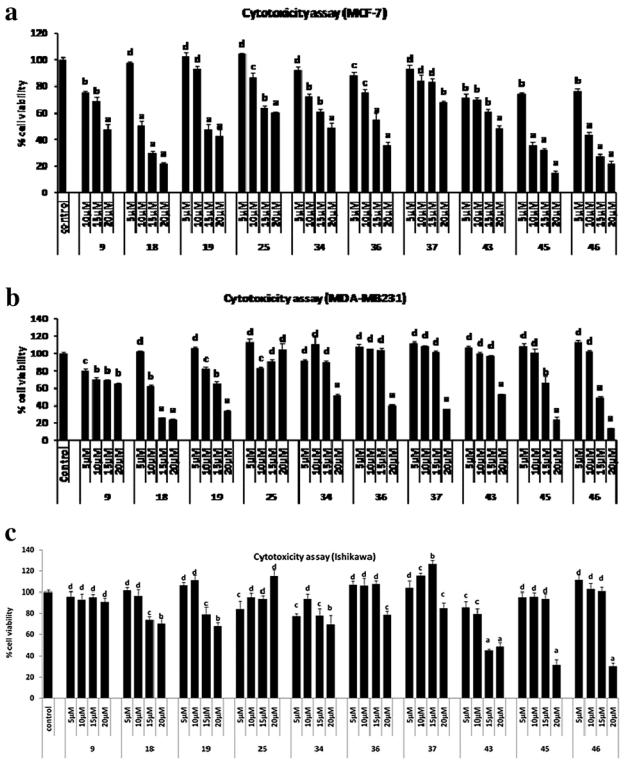

Fig. 2 (a) MTT cell proliferation assay of some active compounds in MCF-7 cells. Results are expressed as mean ± SE, $n = 5$. *P* values are *a* − $p < 0.001$, *b* − $p < 0.01$, *c* − $p < 0.05$, *d* − $p > 0.05$ *vs.* control. (b) MTT cell proliferation assay of some active compounds in MDA-MB 231 cells. Results are expressed as mean ± SE, $n = 5$. *P* values are *a* − $p < 0.001$, *b* − $p < 0.01$, *c* − $p < 0.05$, *d* − $p > 0.05$ *vs.* control. (c) MTT cell proliferation assay of some active compounds in Ishikawa cells. Results are as expressed mean ± SE, $n = 5$. *P* values are *a* − $p < 0.001$, *b* − $p < 0.01$, *c* − $p < 0.05$, *d* − $p > 0.05$ *vs.* control.

all the active compounds, **8–10**, **13–15**, **18**, **19**, **34**, **36**, **43**, **45** and **46**, displayed RBA of <1%. Compounds **20**, **23–24** and **27–28**, with hydroxyl functional groups at the 7th position of the coumarin nucleus, showed good binding affinity. However, the RBA values were drastically reduced with the introduction of a hydroxyl group at the 4′ position of the 3-phenyl ring, as shown in compounds **21–22** and **25–26** (Table 1).

2.2.3. Compounds promote the ALP (alkaline phosphatase) activity of osteoblast cells. The bone specific isoform of alkaline phosphatase, a membrane bound enzyme, is a tetrameric glycoprotein found on the surface of osteoblasts. These cells are responsible for laying down the protein matrix of bone in which calcium salts, particularly phosphates, are deposited. The bone specific alkaline phosphatase is therefore often used as a biochemical marker for osteogenic differentiation/bone turnover. To evaluate if the synthesized compounds increase bone turnover, and later bone formation, we checked the ALP activity of the compounds. Of all the compounds tested, ALP activity was stimulated by five compounds **18** (10 nM), **25** (10 nM, 100 pM), **26** (10 nM, 100 pM), **45** (10 nm, 100 pM), and **46** (10 nM) concentrations (Fig. 3).

17β-Estradiol and raloxifene were used as standard controls, which stimulated ALP activity at 10 nM, 100 nM conc., respectively (Fig. 4). It was observed from the data of this experiment that although the five active compounds have the potential to increase the proliferation and differentiation of osteoblast cells, compared to the positive control only compound **46** showed an increased proliferation comparable to raloxifene. The rest of the four compounds showed no significant change.

2.2.4. Compounds show enhanced osteoblast mineralization *in vitro*. To further assess if the active compounds had the potential for mineralization, which is the final phase in bone formation, we did a mineralization assay, alizarin red-S staining of mineralized nodules (for determining calcium deposition) on 60–70% confluent cells from rat calvaria. The concentration at which compounds showing maximum stimulation of ALP activity were used for assessment of nodule formation or new calcium deposition. Osteoblast cells were treated with the active compounds **18**, **25**, **26**, **45** and **46** and compound treatment was given at doses of 10 nM and 100 pM. At the end of the assay, treated and untreated osteoblasts were fixed and stained with alizarin red-S stain. The data showed that there is an increase in mineralization as compared to the control (not treated cells). Compounds **18**, **25** and **46** at 10 nM concentration and compounds **26** and **45** at 100 pM concentration showed a significant increase in calcium deposition or mineralization compared with the control cells (Fig. 4). Altogether, the data suggests that these compounds have the ability for proliferation, differentiation and mineralization of the osteoblasts, the bone forming cells.

2.2.5. ERα and ERβ-mediated transcriptional activation. The differential response and tissue specific effects by estrogen agonists/antagonists is influenced by their relative affinity for the two ER subtypes, ERα and ERβ and the interactive effects of the estrogen–ER complex with the regulatory proteins. Based on the antiproliferative and antiosteoporotic activities, active compounds **9**, **18**, **19**, **25–28**, **34**, **36**, **37**, **39**, **40**, **43**, **45** and **46** were analysed for their effect on ERE-transcriptional activity in order to explore the ER isoform specific activity and their mechanism of action using ERα and ERβ expression plasmids and the reporter ERE–luciferase plasmid in COS-1 cells.

2.2.6. ERα isoform specific activity. The compounds, when incubated alone, did not significantly affect the ERE–ERα mediated luciferase reporter activity except for compound **28**, which induced the luciferase activity at 20 μM concentration, which also corresponds to the high RBA values of 13.3% for ER. In the presence of estrogen, it was interesting to note that compounds **18**, **19**, **25**, **28**, **45**, and **46** significantly decreased ERE–ERα dependent transcriptional activation in a concentration dependent manner. Among these compounds, **19** appeared to be the most effective in antagonizing the E_2-induced effect at 1 μM, followed by compounds **18** and **46** at 10 μM. The results therefore suggested that the anticancer activity of the above active compounds appeared to be due to the down-regulation of estrogen induced ERα–ERE mediated transactivation caused in different ER +ve cancer cell lines evaluated in this study. The results were comparable with that of tamoxifen, which confirmed that the action of these compounds was mediated *via* the ERα pathway (Fig. 5a and b).

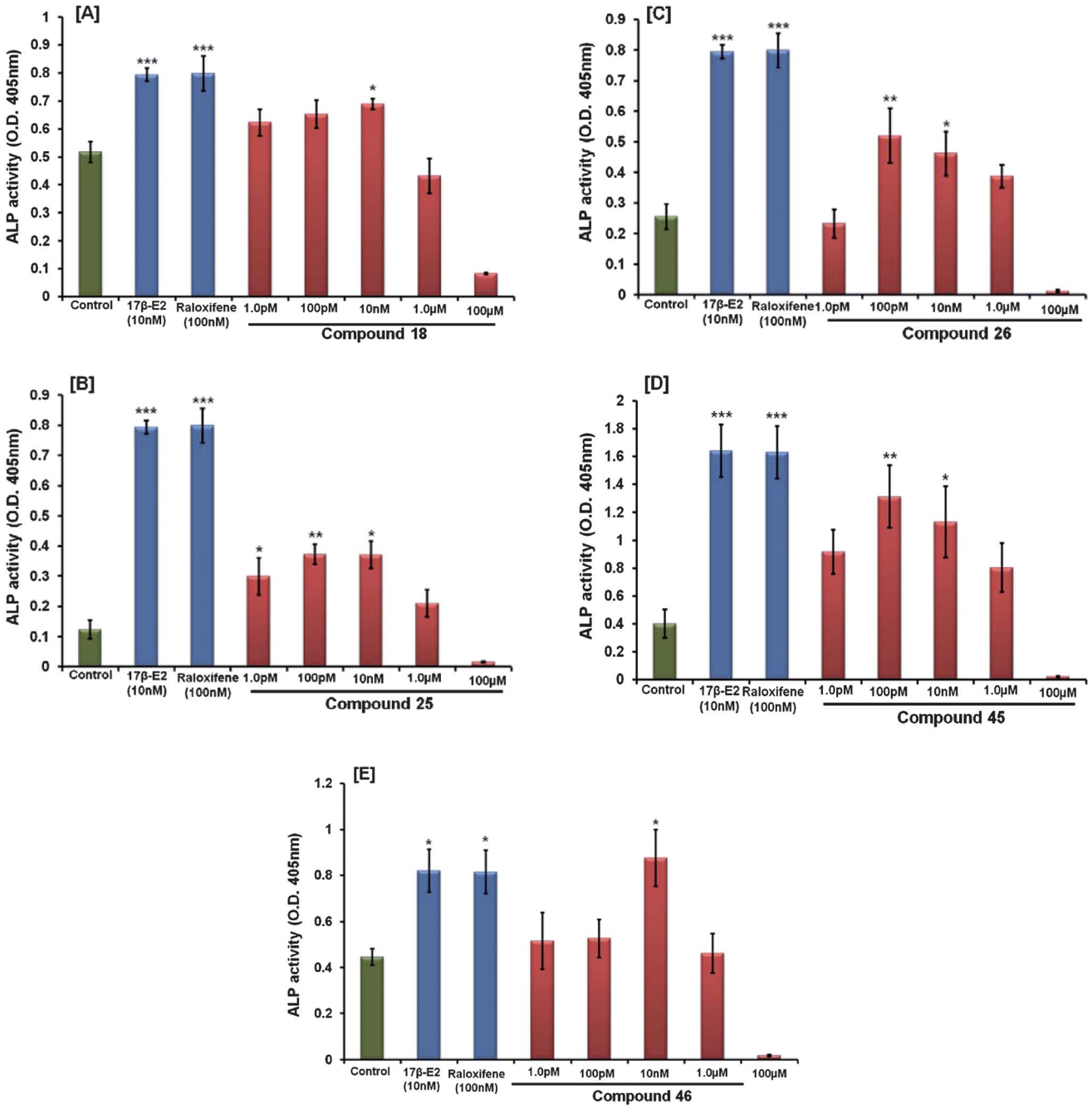

Fig. 3 (A–E) The activity of compounds **18**, **25**, **26**, **45** and **46** were assessed by measuring ALP activity in calvarial osteoblasts (for details see text). At the end of the experiment, ALP activity was measured colorimetrically, as described before. The data shows the mean ± SE of three independent experiments $*p < 0.05$ and $**p < 0.01$.

2.2.7. ERβ isoform specific activity. Evaluation of ERβ isoform specific activity revealed that among the compounds analysed, only five compounds, **19**, **25**, **26**, **45** and **46**, caused the significant induction of ERE–ERβ mediated transcriptional activation, even up to 1 μM. Compounds **18** and **45** induced maximum ERβ activity at 10 μM concentration, whereas **19**, **25** & **45** significantly induced transcriptional activation at 20 μM. These results suggest that the anti-cancer activity of compounds **18**, **19**, **25**, **26** and **46** appeared to be due to upregulation of ERβ functional activity, in addition to the down-regulation of ERα activity caused by these compounds. The upregulation of ERβ activity may be responsible for the significant anti-osteoporotic activity exerted by compounds **18** and **46**. The activity of compound **9** in MCF-7 did not correlate with ER–ERE activity and could probably be acting *via* some other pathway, causing inhibition of the proliferation in MCF-7 cells (Fig. 5c).

2.2.8. Selectivity of ERα and ERβ in action of compounds. To further analyse the specific role of ERα and ERβ in the

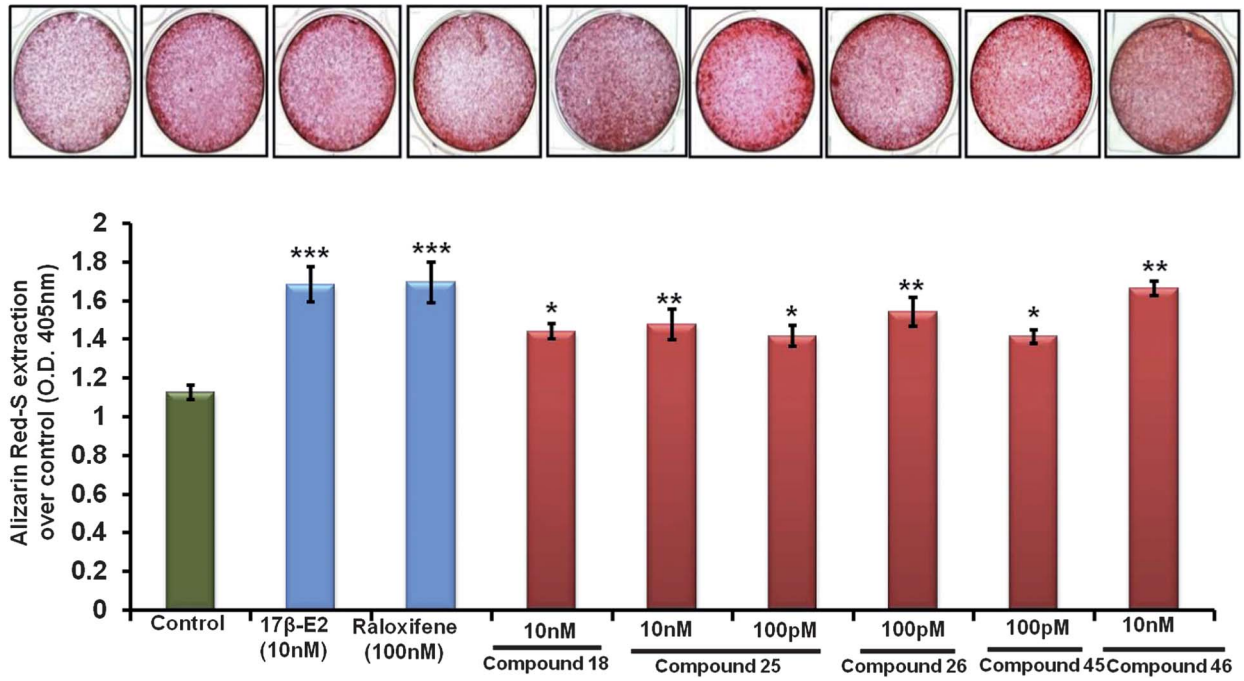

Fig. 4 Compounds **18**, **25**, **26**, **45** and **46** increased osteoblast mineralization. Calvarial osteoblasts were grown in the osteoblast differentiation medium as described before (see text for details). At the end of the experiments, cells were stained with alizarin red-S. Photomicrographs show increased formation of mineralized nodules by compound treatment compared to the vehicle treated cells. The bar diagram shows quantification of mineralization by the extraction of alizarin red-S dye. The data represents the mean ± SE of three independent experiments $*p < 0.05$ and $***p < 0.001$.

anti-proliferative action of these compounds, we transiently knocked down the expression of these proteins using specific SiRNA in MCF-7 breast cancer cells. In cytoxicity assay, ERα SiRNA significantly decreased the proliferation of the MCF-7 cell ($p < 0.01$), shown in Fig. 6(A). Treatment with compounds **18**, **19**, **25**, **28**, **45** and **46** also significantly decreased the viability of the MCF-7 cells. The decrease was not significantly altered when compounds were administered to ERα knockdown cells, indicating that these compounds act *via* inhibition of ERα-mediated signalling. The residual activity could be due to action *via* ERβ. In the case of compound **28**, the ERα SiRNA resulted in increased proliferation of MCF-7 cells. This showed that the anti-proliferative activity of **28** was due to action *via* ERα. In MCF-7 cells with scrambled SiRNA, when incubated with PPT, the ERα agonist, the cell viability was increased, as compared to control normal MCF-7 cells, whereas in MCF-7 cells with ERα SiRNA the agonist activity of PPT was abolished.

As shown in Fig. 6(B), in the presence of ERβ SiRNA, significant induction of cellular proliferation was observed either alone or in presence of compounds **18**, **19**, **25**, **28**, **45** and **46** suggesting the role of ERβ in the action of these compounds. However, it was interesting to note that ERβ knockdown did not significantly alter the decrease in cell viability in the case of compound **28**, demonstrating that this compound acts *via* ERα only and ERβ is not involved in the anti-proliferative action of this compound. These results are in accordance with the results observed in ERα knockdown experiments. In the presence of DPN, the ERβ agonist, cells showed less viability as compared to the control group, which was transfected with scrambled SiRNA.

2.2.9. Assessment of estrogenic and anti-estrogenic activities. Alkaline phosphatase assay in Ishikawa cells was performed to assess the estrogenic and antiestrogenic profiles of active compounds. The results revealed that of the prototype **I** compounds, **9**, **18**, and **25** induced ALP activity at 10 μM and compound **19** at 5 μM concentration, which was further reduced at higher concentration. Compounds **25**, **28**, **36**, **37**, **43**, **45** and **46** did not show estrogenic behavior and compounds **9**, **18**, **19**, **25**, **36**, **37** inhibited ALP activity significantly in a dose dependent manner, which correlates to their anti-proliferative activity against both MCF-7 and MDA-MB 231 breast cancer cell lines. Among the active compounds, the most significant inhibition was observed with compound **46** (Fig. 7).

2.3. Docking protocol

The docking experiments were carried our using the GOLD docking program. For docking studies, the atomic co-ordinates of ERα (PDB id: 1ERR)[30] as well as ERβ (PDBid: 1QKN)[31] were downloaded from the Brookhaven Protein Data Bank (www.rcsb.org) and prepared using the protein preparation wizard implemented in the Schrödinger software package,[32] where bond orders were assigned, water and other residues except bound ligands were deleted, and finally the protein was backbone constrained minimized using OPLS-2005 force field implemented in Schrödinger software package. The bound conformation of the co-crystallized ligands was used in order to define the LBD domain of ERα and ERβ. The optimized 3D-structures of new ligands were docked within a 10 Å radius by

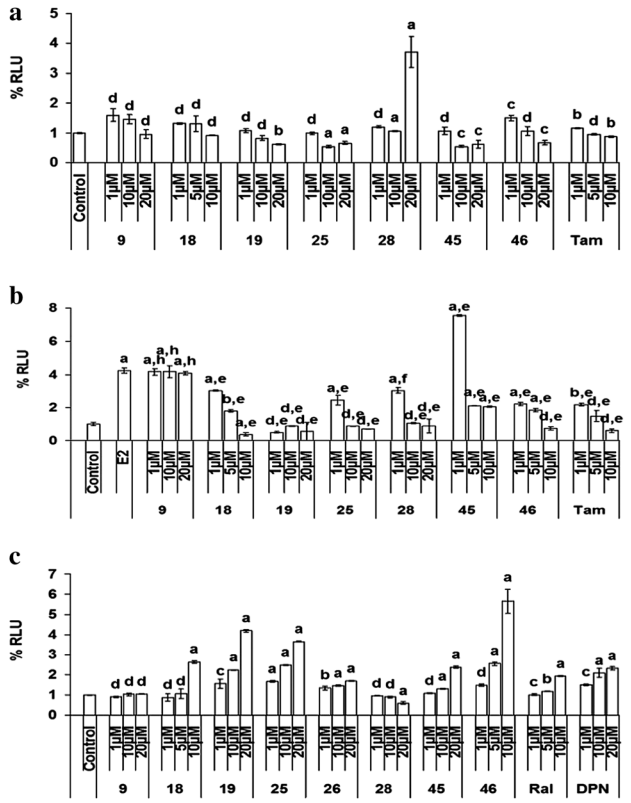

Fig. 5 (a) ERE–ERα-mediated transcriptional activation. (b) ERE–ERα mediated transcriptional activation in the presence of E_2. Transcription activation of compounds *via* ERα–ERE in COS-1 cells in (**6a**) the absence of E_2 and (**5b**) in the presence of 10 nM of E_2. Results are expressed as mean ± SE, $n = 3$. *P* values are $a - p < 0.001$, $b - p < 0.01$, $c - p < 0.05$, $d - p > 0.05$ *vs.* control, $e - p < 0.001$, $f - p < 0.01$, $g - p < 0.05$, $h - p > 0.05$ *vs.* E_2. (c) The effect of compounds on transcription activation *via* ERβ–ERE in COS-1 cells. Results are expressed as mean ± SE, $n = 3$. *P* values are $a - p < 0.001$, $b - p < 0.01$, $c - p < 0.05$, $d - p > 0.05$ *vs.* control.

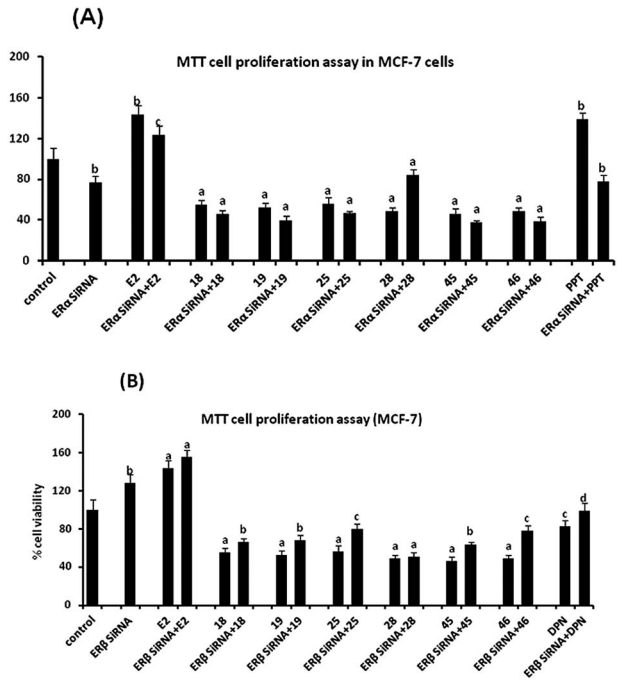

Fig. 6 MCF-7 cells were transiently transfected with ERα (A) or ERβ (B) or non-specific scrambled SiRNA and treated with the compounds for 48 h. Cell viability was measured using MTT cell viability assay. The percentage of viable cells was calculated as the ratio of treated cells to control cells. Results are expressed as mean ± SE, $n = 5$. *p* values are $a - p < 0.001$, $b < 0.01$, $c - p < 0.05$ and $d - p > 0.05$ *vs.* control.

running 20 genetic algorithm (GA) steps for each. The docked poses of geometry optimized ligands were ranked using the GoldScore (GS), to find the most optimal binding pose of each ligand. In the GOLD program, the default parameters: population size (100); selection-pressure (1.1); number of operations (10 000); number of islands (1); niche size (2); and operator weights for migrate (0), mutate (100) and crossover (100) were applied. Finally, the top five binding poses of each ligand were analyzed to select the best binding pose of each ligand in order to untangle the essential parameters in terms of direct- (H-bonds) and indirect (hydrophobic) interactions governing binding disparities among the series of these compounds.

2.3.1. Docking analysis. The differential response and tissue specific effects by estrogen agonist/antagonists is influenced by their relative affinity for the two ER subtypes, ERα, ERβ and the interactive action of the estrogen–ER complex with the regulatory proteins. In the present study, from the biological activity data results of the three prototypes molecules, coumarin derivatives (prototype **I**) exhibited strong antiproliferative activity in both the ER +ve and ER −ve cell lines. Compound **18** and **19**, with methoxy substituents at the *para* position of the two phenyl rings and bearing a pyrrolidino/piperidino alkoxy amino side chain, were found to be the most active, showing a better profile than tamoxifen. This is authenticated by the X-ray crystal structure of **18** (Fig. 8), showing spatial conformation very similar to that of tamoxifen.

The binding site analyses of a number of co-crystallized ER–LBDs have revealed that all of them share a common hydrophobic cavity at the ER–LBD. The ER agonist binding induces a conformational rearrangement in the LBD,[33] resulting in the facilitation of nuclear coactivators binding,[34] while the ER antagonists sterically prevent the correct assembly of the AF-2 region and the NR-box binding cleft.[35] A third category, termed selective ER modulators (SERMS), act both as agonists and antagonists, depending on their tissue locations and the ER isoform.[36] The first SERM tamoxifen (TAM) approved for breast cancer is effective against all stages of breast cancer, whereas raloxifene (RAL) is indicated for the prevention and treatment of osteoporosis in postmenopausal women.[37] These SERMs have beneficial effects on bone and lipid metabolism while antagonizing the effects of estrogens on the uterus and breasts.

In the present study molecular docking was performed through the GOLD[38] docking program to gain insight into the probable nature of the binding and to understand the activity variation among the highly active representatives (compound **18** and **45**) of synthesized prototypes, as well as the least active compound (compound **20**) reported herein, along with the

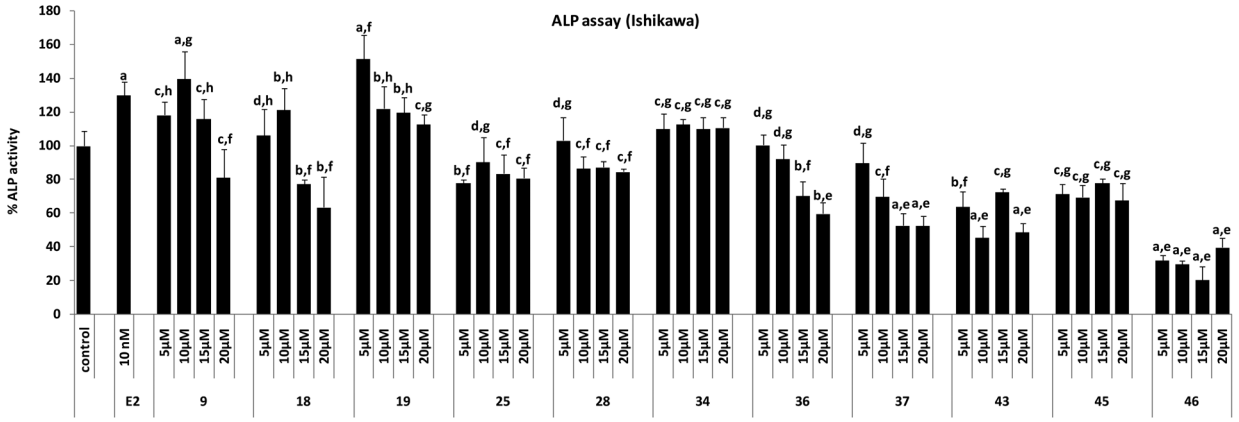

Fig. 7 ALP assay in Ishikawa cells. Results are expressed as mean ± SE, $n = 5$. P values are $a - p < 0.001$, $b - p < 0.01$, $c - p < 0.05$, $d - p > 0.05$ *vs.* control, $e - p < 0.001$, $f - p < 0.01$, $g - p < 0.05$, $h - p > 0.05$ *vs.* E_2.

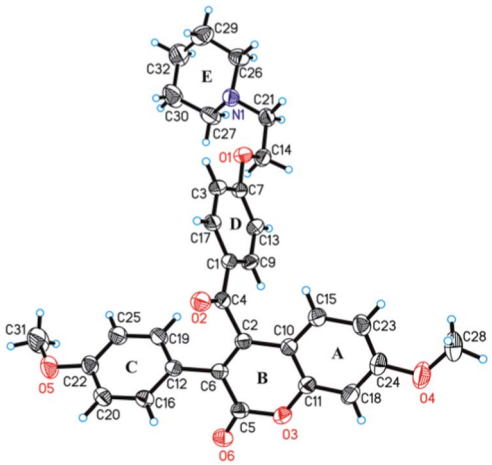

Fig. 8 ORTEP diagram (at 30% probability) of **18**, along with atomic numbering scheme for the non-hydrogen atoms.

control drug RAL (to date RAL is the only SERM that has been co-crystallized with both ERs, the ERα (PDB id: 1ERR) and ERβ (PDB id: 1QKN)) and TAM at the LBD domain of ERα as well as ERβ.

2.3.2. Docking to the LBD domain of ERα. The human ERα (PDB ID: 1ERR), co-crystallized with the RAL, was chosen for the molecular docking studies. Protein was prepared using the protein preparation wizard implemented in the Schrödinger software package, and the active site of the protein was defined using the co-crystallized ligand RAL. The ligands were minimized using the OPLS-2005 force field implemented in the Schrödinger software package. Fig. 9A depicts the binding pose comparison of the well known ERα antagonist RAL with TAM at the LBD domain, where it can be observed that TAM and RAL follow a similar binding pattern. Similarly, the binding pose comparison of most active molecules of the series (compound **18**; IC_{50}: 0.16 μM) with a coumarin core showed that the binding pattern of this molecule is nearly identical to RAL (Fig. 9B). The coumarin core nucleus of **18** occupied the hydrophobic cavity made by the residues Glu353, Arg394, Phe404 and Leu349, while the methoxy group attached to the coumarin moiety interacts with the residues Glu353 and Arg394. The 4-methoxyphenyl group attached at the 3rd position of the coumarin nucleus occupied the hydrophobic cavity made by the residues Met421, Gly521, His524, Leu346 and Ile424. The aroyl substituent with the basic aminoalkoxy chain at the 4th position of compound **18** is anchored by compact hydrophobic contacts, made by residues Trp383, Asp351, Leu 354, Leu536 and Thr347 around the piperidine ring. The length of the side chain of compound **18** is nearly superimposable over that of RAL, displaces the H12 more efficiently and protrudes from the pocket between H3 and H11, thereby resulting in higher ERα antagonism than RAL. Next, the binding pattern of compound **18** (prototype **I**, IC_{50}: 0.16 μM), compared with the most active compound **45** (prototype **III**, IC_{50}: 0.22 μM), with dimethyl chromene as a common core at the LBD domain, is shown in Fig. 9C. The compound **45** showed a very different binding orientation from the RAL, as in this molecule the aminoalkoxy side chain is for the first time linked at the 6th position (benzene ring) of the chromene pharmacophore (whereas almost all SERMs reported to date invariably contain the side chain linked to the aryl ring attached to the heterocyclic ring).

The binding analysis of compound **45** showed that the chromene moiety of the molecule occupied the hydrophobic cavity made by the residues Phe404, Leu391, Met388, and Glu353, while the phenyl group linked with the chromene moiety is accommodated in the cavity made by the residues Met421, His524, Gly521, Ile424 and Leu428. The binding cavity of the aroyl chromene core of compound **45** occupied the hydrophobic space similar to RAL but less efficiently (cavity diagonally across the cavity between H11, H3 and H6). However, this less efficient hydrophobic occupancy has been compensated by the H-bond interaction of ketonic oxygen attached to the chromene moiety. The side chain of compound **45**, though, showed a different orientation than the side chain orientation of compound **18** and RAL but it efficiently displaces the H12 and protrudes from the pocket between H3 and H11, resulting in ER antagonism better than RAL and comparable to compound **18** (Fig. 10C). The weak antagonism/activity of compound **20** can

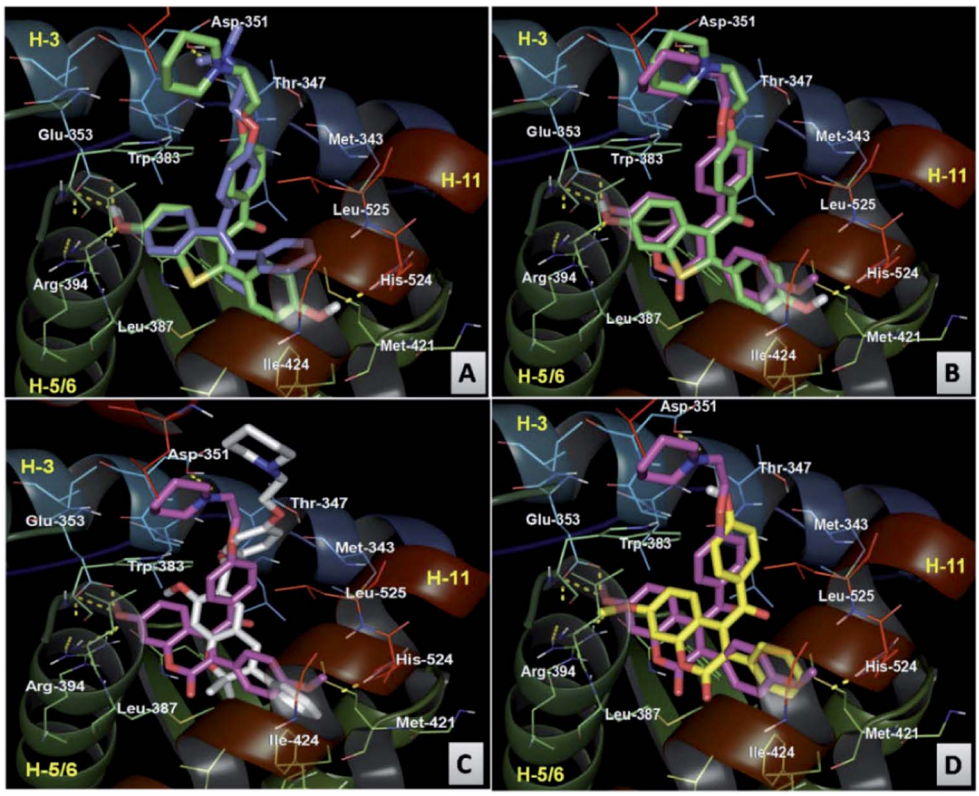

Fig. 9 Comparative 3D binding view of (A) RAL (green carbon) and TAM (blue carbon) (B), RAL (green carbon) and compound **18** (pink carbon) (C), compound **18** (pink carbon) and compound **45** (white carbon) (D) compound **18** (pink carbon) and compound **20** (yellow carbon) at the LBD domain of ERα.

be easily explained by the absence of the aminoalkoxy side chain, thereby resulting in the non-displacement of H12 (Fig. 9D).

2.3.3. Docking to the LBD domain of ERβ. The human ERβ (PDB ID: 1U3Q) co-crystallized with the ligand **CL-272** was chosen for the molecular docking studies, since the co-crystallized structure of RAL with human ERβ is unknown, although the crystal structure of the LBD domain of rat ERβ is known. Keeping this in view, initially RAL was docked at the LBD domain of human ERβ and was compared with its binding at the LBD domain of rat ERβ to ensure the correct binding of the ligands. The protein was prepared using the protein preparation wizard implemented in the Schrödinger software package and the active site of the protein was defined using the co-crystallized ligand RAL. The ligands were minimized using OPLS-2005 force field implemented in the Schrödinger software package.

A comparison of the binding of RAL with TAM in ERβ binding cavity revealed both compounds comparably accommodated in the same manner, as observed in the ERα complex (Fig. 10A). Furthermore, it was also observed that compound **18** in ERβ followed a similar binding pattern to RAL (Fig. 10B). The basic pharmacophore, made of a coumarin core (compound **18**), occupied the hydrophobic cavity made by the residues Glu305, Arg346, Leu301, Leu339, and Leu343, which were different from the amino acid residues as observed in ERα. The 4-methoxyphenyl group attached at the 4th position of the coumarin nucleus occupied the hydrophobic cavity made from the residues Met421, Gly472, His575, Leu298, Phe356, Met340, Ile376 and Ile373, the characteristic amino acid residue for ERβ affinity. The side chain of compound **18** is anchored by hydrophobic contacts made by residues Leu476, Leu495, Leu306, Met494, Trp335, and Leu491 around the piperidine ring. However, the length of the side chain of compound **18** is almost superimposable on the side chain of RAL, efficiently displacing the H12, and protrudes from the pocket between H3 and H11, giving credence to the partial agonism and antagonism (SERM like behavior) shown by compound **18**. Next, a comparative binding study of compound **18** with that of compound **45** at the LBD domain of ERβ (Fig. 10C) revealed that the binding orientation of the side chain of compound **45** is slightly moved towards H11, compared to its binding orientation as observed in the ERα complex; still it efficiently displaces H12 and protrudes from the pocket between H3 and H11. This explains its ER antagonism being better than that of RAL and comparable to that of compound **18**. The aroylchromene cores of the molecule occupy a similar hydrophobic space, diagonally across the cavity between H11, H3 and H6, as observed in the ERα complex. The binding orientation of the non active compound **20** in the binding domain of ERβ was the same as that observed in the ERα complex (Fig. 10D). The key observation is that the

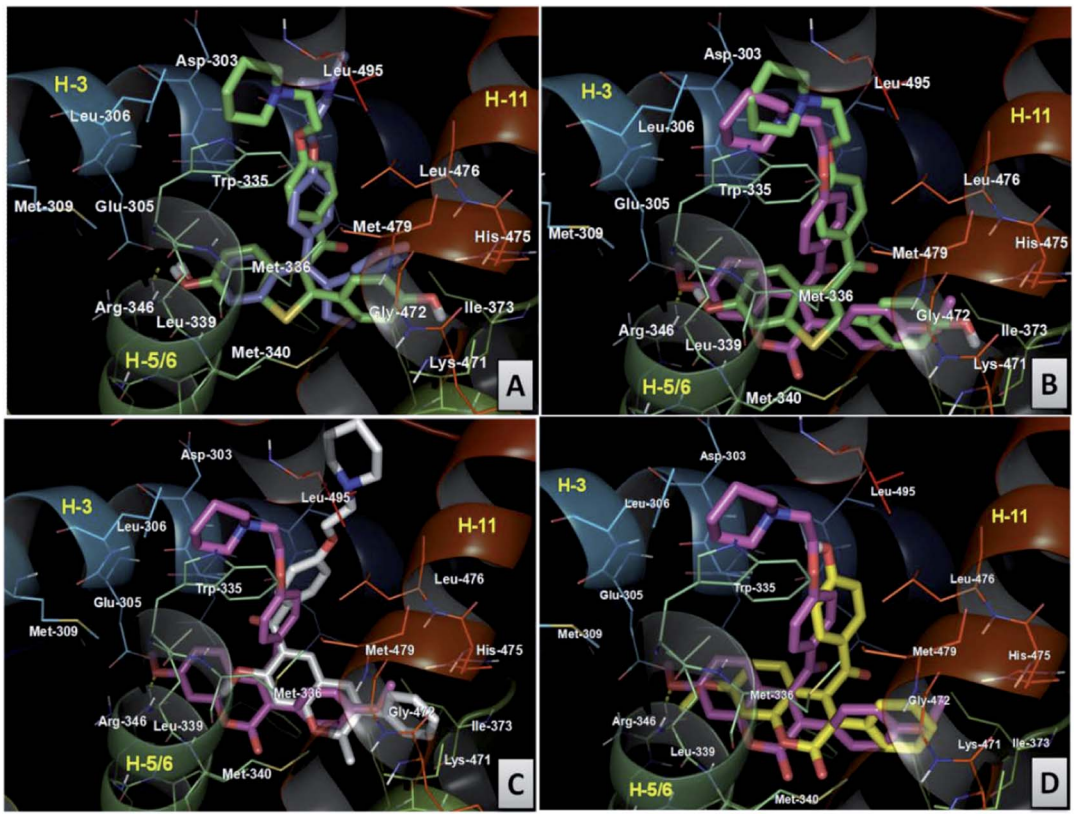

Fig. 10 Comparative 3D binding view of (A) RAL (green carbon) and TAM (blue carbon) (B), RAL (green carbon) and compound **18** (pink carbon) (C), compound **18** (pink carbon) and compound **45** (white carbon) (D) compound **18** (pink carbon) and compound **20** (yellow carbon) at the LBD domain of ERβ.

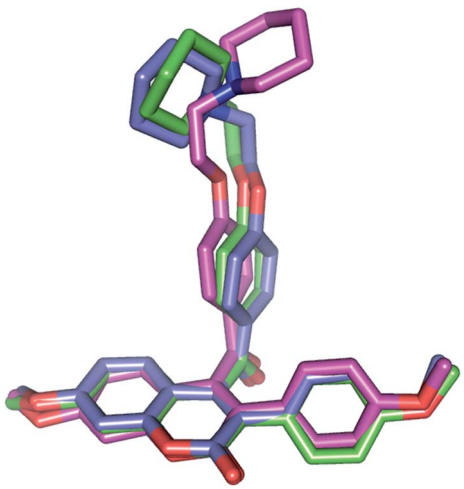

Fig. 11 Comparison of conformation for the compound **18** in the crystallized form (pink colored carbon) with docked conformation at the ERα (green colored carbon) and ERβ (blue colored carbon) binding site.

binding orientation of the side chain of compound **45** in ERβ is different from that of **18** and RAL; it induces maximum ERβ specific activity and thereby enhances bone specific osteoblast differentiation at 100 pM.

2.3.4. Comparison of the crystallized state of compound 18 with its docked state at the LBD domain of ERα and ERβ. In order to evaluate the similarity between the crystallized conformation and the bioactive conformation, a comparative study has been performed between the crystallized conformation and the docked conformation of compound **18** at the ERα and ERβ active sites (Fig. 11). The comparison study revealed that the docked conformations of compound **18** at the ERα and ERβ active sites were more or less superimposable on each other. Furthermore, the crystallized conformation (pink colored carbon) was also in good agreement with the docked conformation of compound **18**, where the arylcoumarin cores exactly superimposed on one another. The side chain of the crystallized conformation moved a little apart from the docked conformation, while the nitrogen of piperidine occupied the same space. This side chain movement of the docked conformation may be due to strong hydrophobic forces, which led the molecule to occupy the space diagonally across the cavity between H11, H3 and H6 in the ERα and ERβ complex.

3. Conclusions

In conclusion, it can be clearly seen that the carbon chain of active compounds **18** and **45** is oriented perpendicular to the bicyclic coumarin/chromene pharmacophore, giving the favorable conformation shown by most of the estrogen antagonists.

Docking of **18** in the ligand binding cavity of ERα, showed that the molecule favorably fits in the ligand binding space and makes hydrophobic interactions with the salient amino acids (Glu353, Arg394, His524) known to anchor both the estrogenic and antiestrogenic ligands in the binding pocket of LBD, and the side chain is projected towards Asp351. In prototype **II** molecules, where the carbonyl functional group is reduced to methylene (CH_2), due to weak hydrophobic interactions biological activity is substantially decreased. This reinforces the hypothesis that a polar atom or a substituent is an essential requisite for making hydrophobic contacts within the receptor pocket and the potential biological efficacy. The surprise discovery of the present study is the novel prototype **III** molecules **45** & **46** with aroyl substitution at the 6th position. Both the compounds have shown potent antiproliferative activity against both the breast cancer cell lines, promote alkaline phosphatase activity, enhance osteoblast mineralization *in vitro*, significantly decrease ERE–ERα dependent transactivation and induce ERβ activity. The upregulation of ERβ specific isoform activity of **45** may be responsible for the antiosteoporotic activity of this molecule at picomolar concentrations. In addition, both the compounds were also devoid of any estrogenic activity, which correlates to their antiestrogenic behaviour in the two breast cancer cell lines.

4. Experimental

4.1. Materials and methods

All the glass apparatus was oven dried prior to use. All chemicals and reagents were purchased from Sigma-Aldrich or ACROS ORGANICS and were used without further purification. Solvents THF, DCM, DMF, DMSO, diethyl ether, acetone were purified using standard methods. 100–200 mesh silica gel was used for column chromatography, and TLC was performed on Merck-precoated silica gel 60-F_{254} and aluminum oxide 60-F_{254} plates. Melting points were recorded with COMPLAB melting point apparatus and are uncorrected. The chromatographic solvents are mentioned as v/v ratios. All the synthesized compounds were fully characterized by ^{1}H, ^{13}C NMR, IR, and further confirmed through ESI-MS, ESI-HRMS analysis. IR spectra were recorded on a Perkin-Elmer FT-IR RXI spectrophotometer and the values were reported in cm^{-1}. ^{1}H NMR and ^{13}C NMR spectra were recorded on Bruker DRX-300 (300 MHz for ^{1}H) and at 75 MHz for ^{13}C or DPX-200 (at 50 MHz for ^{13}C) spectrometers using $CDCl_3$, DMSO-d_6, CD_3OD or acetone-d_6 as solvents using tetramethylsilane as the internal standard. Chemical shifts are reported in parts per million. ESI-MS spectra were obtained on a LCQ Advantage Ion trap mass spectrometer (Finnigan thermo Fischer scientific) and High-resolution mass spectra (ESI-HRMS) were recorded on an Agilent 6520 ESI-QTOP mass spectrometer. All products reported showed ^{1}H NMR and ^{13}C NMR spectra in agreement with the assigned structures. The purity of compounds was determined by HRMS, and all tested compounds yielded data consistent with a purity of at least 95% as compared with the theoretical values.

*1-(2-Hydroxy-4-methoxyphenyl)-2-(4-hydroxyphenyl)ethane-1,2-dione (compound **5**).* Yellow solid, mp 172 °C; IR (KBr) ν 3342, 1652, 1623 1525, cm^{-1}; ^{1}H NMR (300 MHz, DMSO d_6) δ 11.00 (s, 1H), 10.61 (s, 1H), 7.68 (d, J = 8.41 Hz, 3H), 23 (m, 2H), 6.90 (d, J = 8.5 Hz, 2H); 6.61–6.57 (m, 1H) 6.41 (d, J = 1.92 Hz, 1H); ^{13}C NMR (50 MHz), 195.0, 166.9, 163.5, 132.4, 132.2, 127.5, 124.8, 116.2, 114.2, 108.4, 101.2, 56.1. ESI-MS: (m/z) 273 [M + H].$^+$

Coumarins **8–11** were synthesised following the representative procedure as described for compound **8** and compounds **12–19** were synthesized by using same procedure described for compound **12**.

4.1.1. Representative procedure for the synthesis of compounds 8–11

*Synthesis of 4-(4-hydroxybenzoyl)-3-phenyl-2H-chromen-2-one (compound **8**).* To a stirred solution of benzil **3** (0.726 g, 3 mmol) in anhydrous acetone (20 ml) was added anhydrous K_2CO_3 (0.690 g, 5 mmol) followed by slow addition of phenylacetyl chloride (0.541 g, 3.5 mmol). The reaction mixture was then stirred vigorously at 80 °C for 4 h. After completion of the reaction, excess solvent was removed under vacuum and 5% aq. cold HCl (30 ml) was added. The solid precipitate was filtered, washed with water, dried and crystallized from diethyl ether to afford a white crystalline compound; yield: 0.923 g, 95%; mp 168 °C; IR (KBr) ν 3208, 1684, 1656 1595, cm^{-1}; ^{1}H NMR (300 MHz, $CDCl_3$ + acetone d_6) δ 7.61 (d, J = 8.7 Hz, 2H), 7.51–7.45 (m, 1H), 7.33 (d, J = 8.1 Hz, 1H) 7.27–7.23 (m, 2H), 7.20–7.11 (m, 5H), 6.70 (d, J = 8.7 Hz, 2H); ^{13}C NMR (50 MHz, DMSO-d_6) δ 191.2, 163.6, 159.8, 152.9, 148.2, 132.9, 132.3, 132.0, 129.7, 128.4, 127.7, 126.4, 126.0, 124.7, 117.4, 116.7, 115.7; ESI-MS: (m/z) 343 [M + H]+; HRMS-ESI: [M + H]$^+$ for $C_{22}H_{15}O_4$ calcd 343.0970; found 343.0965%.

*4-(4-Hydroxybenzoyl)-7-methoxy-3-phenyl-2H-chromen-2-one (compound **9**).* In accordance to general procedure benzil **5** and phenylacetyl chloride were used as reactants; white solid; yield: 1.06 g, 95%; mp 174 °C; IR (KBr) ν 3238, 1689, 1594, 1506,cm^{-1}; ^{1}H NMR (300 MHz, DMSO-d_6) δ 10.65 (hump, 1H), 7.73 (d, J = 8.7 Hz, 2H) 7.26–7.22 (m, 5H), 7.14 (d, J = 2.3 Hz, 1H), 7.06 (d, J = 8.8 Hz, 1H), 6.89 (dd, J = 8.8, 2.3 Hz, 1H), 6.73 (d, J = 8.7 Hz, 2H), 3.87 (s, 3H); ^{13}C NMR (DMSO-d_6, 75 MHz), δ 191.9, 164.0, 162.9, 155.3, 149.0, 133.6, 132.8, 130.4, 128.6, 128.2, 127.6, 126.9, 121.7, 116.2, 113.2, 111.3, 101.6, 56.5; ESI-MS: (m/z) 372; found 373 [M + H]$^+$; HRMS-ESI: [M + H]$^+$ for $C_{23}H_{16}O_5$ calcd 373.1076; found 373.1066%.

*4-(4-Hydroxybenzoyl)-3-(4-methoxyphenyl)-2H-chromen-2-one (compound **10**).* In accordance to general procedure benzil **3** and 4-methoxy phenylacetyl chloride were used as reactants; white solid; yield: 1.004 g, 90%; mp 162 °C; IR (KBr) ν 3278, 1691, 1651, 1602, 1577, cm^{-1}; ^{1}H NMR (300 MHz, DMSO-d_6) δ 7.73 (d, J = 8.7 Hz, 2H), 7.66–7.60 (m, 1H), 7.51 (d, J = 7.6 Hz, 1H), 7.30–7.21 (m, 3H), 7.15–7.12 (m, 1H), 6.82 (d, J = 8.8 Hz, 2H), 6.70 (d, J = 8.7 Hz, 2H), 3.69 (S, 3H); ^{13}C NMR (DMSO-d_6, 75 MHz) δ 191.7, 165.0, 160.5, 159.7, 153.2, 148.2, 132.8, 132.3, 131.7, 126.4, 126.3, 125.5, 125.2, 124.8, 118.1, 117.2, 116.4, 113.7, 55.5; ESI-MS: (m/z) 372; found, 373 [M + H]$^+$; HRMS-ESI: [M + H]$^+$ for $C_{23}H_{17}O_5$ calcd 373.1076; found 373.1057%.

*4-(4-Hydroxybenzoyl)-7-methoxy-3-(4-methoxyphenyl)-2H-chromen-2-one (compound **11**).* In accordance with general procedure benzil **5** and 4-methoxy phenylacetyl chloride were used as reactants; yellow solid; yield: 1.08 g, 90%; mp 180 °C, IR (KBr) ν 3221, 1686, 1646, 1592, 1509, cm^{-1}; ^1H NMR (300 MHz, DMSO-d_6) δ 7.73 (d, J = 8.7 Hz, 2H), 7.20 (d, 8.7 Hz, 2H), 7.12 (d, J = 2.3 Hz, 1H), 7.03 (d, J = 8.8 Hz, 1H), 6.88 (dd, J = 8.8, 2.4 Hz, 1H), 6.80 (d, J = 8.7 Hz, 2H), 6.73 (d, J = 8.7 Hz, 2H), 3.86 (s, 3H), 3.68 (s, 3H); ^{13}C NMR (DMSO-d_6, 75 MHz), δ 192.1, 164.1, 162.7, 160.8, 159.5, 155.1, 148.5, 132.82, 131.7, 127.5, 126.9, 125.6, 121.4, 116.2, 113.7, 111.4, 101.5, 56.5, 55.4; ESI-MS (m/z): 402; found 403 $[M + H]^+$; HRMS-ESI: $[M + H]^+$ for $C_{24}H_{19}O_6$ calcd 403.1182; found 403.1054%.

4.1.2. Representative procedure for the synthesis of compounds 12–19

*Synthesis of 3-phenyl-4-(4-(2-(piperidin-1-yl)ethoxy)benzoyl)-2H-chromen-2-one (compound **12**).* To the stirred solution of compound **8** (0.513 g, 1.5 mmol) in dry acetone (20 ml) anhydrous K_2CO_3 (0.690 g, 4.5 mmol) and 1-(2-chloroethyl) piperidine hydrochloride (0.322 g, 1.75 mol) were added. The reaction mixture was refluxed with stirring until complete consumption of the starting material. The excess solvent was removed under vacuum and cold water (30 ml) was added to the residue. It was extracted with DCM (20 ml × 3) and the combined organic layers were dried over Na_2SO_4. The crude product obtained on removal of the solvent was purified by chromatography on a silica gel column (chloroform : methanol 50 : 1) to give a white crystalline solid; yield: 0.625 g, 92%; mp 180 °C; IR (KBr) ν 1725, 1658, 1598, cm^{-1}; ^1H NMR (300 MHz, $CDCl_3$) δ 7.74 (d, J = 8.8 Hz, 2H), 7.59–7.54 (m, 1H), 7.45 (d, J = 8.2 Hz, 1H), 7.37–7.34 (m, 2H), 7.30–7.19 (m, 5H), 6.82 (d, J = 8.8 Hz, 2H) 4.11 (t, J = 5.9 Hz, 2H), 2.74 (t, J = 5.9 Hz, 2H), 2.48 (t, J = 4.8 Hz, 4H) 1.62–1.58 (m, 4H), 1.45 (m, 2H); ^{13}C NMR ($CDCl_3$, 75 MHz), δ 192.1, 163.9, 160.5, 153.4, 148.9, 132.4, 131.41, 131.8, 129.9, 128.9, 126.5, 124.7, 117.8, 117.0, 114.7, 66.4, 57.6, 55.0, 29.7, 25.8, 24.0; ESI-MS (m/z): 453; found 454 $[M + H]^+$; HRMS–ESI; $[M + H]^+$ for $C_{29}H_{28}NO_4$ calcd 454.2018; found 454.2006%.

*3-Phenyl-4-(4-(2-(pyrrolidin-1-yl)ethoxy)benzoyl)-2H-chromen-2-one (compound **13**).* Compound **8** and 1-(2-chloroethyl) pyrrolidine hydrochloride were used as reactants; white solid; yield: 0.593 g, 90%; mp 186 °C; IR (KBr) ν, 1722, 1659, 1597, 1424 cm^{-1}; ^1H NMR (300 MHz, $CDCl_3$) δ 7.73 (d, J = 8.7, 2H), 7.59–7.55 (m, 1H), 7.45 (d, J = 8.1 Hz, 1H), 7.34–7.28 (m, 2H), 7.24–7.19 (m, 5H), 6.84 (d, J = 8.7 Hz, 2H), 4.11 (t, J = 5.7 Hz, 3H), 2.88 (t, J = 5.7 Hz, 2H), 2.60 (m, 4H), 1.80 (m, 4H); ^{13}C NMR ($CDCl_3$, 75 MHz), δ 192.1, 163.9, 153.4, 148.9, 132.4, 131.9, 131.8, 129.9, 128.8, 128.3, 128.1, 126.53, 125.2, 124.7, 117.8, 117.0, 114.6, 67.5, 54.7, 23.5; ESI-MS (m/z): 439; found 440 $[M + H]^+$; HRMS-ESI: $[M + H]^+$ for $C_{28}H_{26}NO_4$ calcd 440.1862; found 440.1844%.

*7-Methoxy-3-phenyl-4-(4-(2-(piperidin-1-yl)ethoxy)benzoyl)-2H-chromen-2-one (compound **14**).* Compound **9** and 1-(2-chloroethyl) piperidine hydrochloride were used as reactants. Creamy solid; yield: 0.689 g, 95%; mp 192 °C; IR (KBr) ν, 1714, 1653, 1603, 1509, cm^{-1}; ^1H NMR (300 MHz, $CDCl_3$) δ 7.73 (d, J = 8.8 Hz, 2H), 7.35–7.32 (m, 2H), 7.26–7.16 (m, 4H), 6.94 (d, J = 2.4 Hz, 1H), 6.82–6.76 (m, 3H), 4.10 (t, J = 6.0 Hz, 2H), 3.89 (s, 3H), 2.74 (t, J = 5.9 Hz, 2H), 2.48 (t, J = 4.8 Hz, 4H) 1.63–1.56 (m, 4H), 1.48–1.45 (m, 2H); ^{13}C NMR ($CDCl_3$, 75 MHz) δ 192.3, 163.9, 162.9, 160.9, 155.2, 149.2, 132.7, 131.8, 130.0, 128.5, 128.1, 127.5, 121.8, 114.6, 112.9, 111.3, 100.9, 66.4, 57.61, 55.5, 55.1, 25.8, 24.1; ESI-MS (m/z): 483; found 484 $[M + H]^+$; HRMS-ESI: $[M + H]^+$ for $C_{30}H_{30}NO_5$ calcd 484.2124; found 484.2116%.

*7-Methoxy-3-phenyl-4-(4-(2-(pyrrolidin-1-yl)ethoxy)benzoyl)-2H-chromen-2-one (compound **15**).* Compound **9** and 1-(2-chloroethyl) pyrrolidine hydrochloride were used as reactants; creamy solid; yield: 0.634 g, 90%; mp 188 °C; IR (KBr) ν, 1713, 1653, 1603, 1508, cm^{-1}; ^1H NMR (300 MHz, $CDCl_3$) δ 7.75 (dd, J = 8.9, 2.6 Hz, 2H), 7.36–7.30 (m, 2H), 7.25–7.18 (m, 4H), 6.95 (d, J = 2.5 Hz, 1H), 6.86–6.78 (m, 3H), 4.13 (t, J = 5.6 Hz, 2H), 3.91 (s, 3H), 2.91 (t, J = 3.0 Hz, 2H), 2.62 (m, 4H) 1.82 (m, 4H); ^{13}C NMR ($CDCl_3$, 75 MHz) δ 192.4, 163.9, 162.9, 161.0, 155.3, 149.2, 132.7, 131.7, 130.0, 128.6, 128.4, 127.5, 121.8, 114.6, 112.95, 111.3, 101.0, 67.5, 55.8, 54.7, 29.7, 23.50; ESI-MS (m/z):469; found 470 $[M + H]^+$; HRMS-ESI: $[M + H]^+$ for $C_{29}H_{28}NO_5$ calcd 470.1967; found = 470.1975%.

*3-(4-Methoxyphenyl)-4-(4-(2-(piperidin-1-yl)ethoxy)benzoyl)-2H-chromen-2-one (compound **16**).* Compound **10** and 1-(2-chloroethyl) piperidine hydrochloride were used as reactants; creamy solid; yield: 0.689 g, 95%; mp 190 °C; IR (KBr) ν, 1720, 1655, 1598, 1570, 1511, cm^{-1}; ^1H NMR (300 MHz, $CDCl_3$) δ 7.75 (d, J = 8.6 Hz, 2H), 7.56–7.51 (m, 1H), 7.43 (d, J = 8.1 Hz, 1H), 7.32–7.26 (m, 3H), 7.23–7.20 (m, 1H), 6.82 (d, J = 8.7 Hz, 2H), 6.77 (d, J = 8.6 Hz, 2H), 4.10 (t, J = 5.7 Hz, 2H), 3.74 (s, 3H) 2.74 (t, J = 5.7 Hz, 2H), 2.48 (m, 4H), 1.59–1.57 (m, 4H); 1.46–1.44 (m, 2H); ^{13}C NMR ($CDCl_3$, 75 MHz), δ 192.4, 163.9, 160.8, 159.9, 153.3, 148.1, 131.8, 131.6, 131.4, 128.2, 126.3, 12 4.9, 124.7, 118.0, 116.9, 114.7, 113.6, 66.5, 57.6, 55.1, 25.9, 24.1; ESI MS (m/z): 483; found 484 $[M + H]^+$; HRMS-ESI: $[M + H]^+$ for $C_{30}H_{30}NO_5$ calcd 484.2124; found 484.2229%.

*3-(4-Methoxyphenyl)-4-(4-(2-(pyrrolidin-1-yl)ethoxy)benzoyl)-2H-chromen-2-one (compound **17**).* Compound **10** and1-(2-chloroethyl) pyrrolidine hydrochloride were used as reactants. Creamy solid; yield: 0.633 g, 90%; mp 186 °C; IR (KBr) ν, 1721, 1652, 1597, cm^{-1}; ^1H NMR (300 MHz, $CDCl_3$) δ 7.75 (d, J = 8.7 Hz, 2H), 7.56–7.52 (m, 1H), 7.43 (d, J = 8.1 Hz, 1H), 7.32–7.26 (m, 3H), 7.22–7.20 (m, 1H), 6.84 (d, J = 8.7 Hz, 2H), 6.77 (d, J = 8.6 Hz, 2H), 4.11 (t, J = 5.6 Hz, 2H), 3.74 (s, 3H) 2.89 (t, J = 5.7 Hz, 2H), 2.61 (m, 4H), 1.80 (m, 4H); ^{13}C NMR ($CDCl_3$, 75 MHz) δ 192.41, 163.94, 160.89, 159.89, 153.25, 148.17, 131.86, 131.69, 131.37, 128.27, 126.37, 124.90, 124.72, 124.66, 117.98, 116.97, 114.70, 113.69, 67.49, 55.15, 54.74, 30.89, 23.49; ESI-MS (m/z): 469; found 470 $[M + H]^+$; HRMS-ESI: $[M + H]^+$ for $C_{29}H_{28}NO_5$ calcd 470.1967; found 470.1982%.

*7-Methoxy-3-(4-methoxyphenyl)-4-(4-(2-(piperidin-1-yl) ethoxy)-benzoyl)-2H-chromen-2-one (compound **18**).* Compound **11** and 1-(2-chloroethyl) piperidine hydrochloride were used as reactants; white solid; yield: 0.731 g, 95%; mp 210 °C; IR (KBr) ν, 1726, 1652, 1602, 1508, cm^{-1}; ^1H NMR (300 MHz, $CDCl_3$) δ 7.73 (d, J = 8.7 Hz, 2H), 7.27 (d, J = 8.5 Hz, 2H), 7.16 (d, J = 8.8 Hz, 1H), 6.91 (d, J = 2.0 Hz, 1H), 6.83–6.74 (m, 5H), 4.10 (t, J = 5.6 Hz, 2H), 3.88 (s, 3H), 3.72 (s, 3H), 2.74 (t, J = 5.7, 2H), 2.48 (m, 4H) 1.59–1.57 (m, 4H); 1.46–1.44 (m, 2H); ^{13}C NMR ($CDCl_3$, 75 MHz) δ 192.6, 163.8, 162.7, 161.2, 159.6, 155.0, 148.4, 131.8, 131.3,

128.2, 127.3, 124.9, 121.5, 114.6, 113.6, 112.8, 111.4, 100.9, 66.40, 5.60, 55.8, 55.1, 55.0, 30.8, 25.8, 24.0; ESI-MS (*m*/*z*): 513; found 514 $[M + H]^+$; HRMS-ESI: $[M + H]^+$ for $C_{31}H_{32}NO_6$ calcd 514.2230; found 514.2231%.

*7-Methoxy-3-(4-methoxyphenyl)-4-(4-(2(-pyrrolidin-1-yl) ethoxy)-benzoyl)-2H-chromen-2-one (compound **19**).* Compound **11** and 1-(2-chloroethyl) pyrrolidine hydrochloride were used as reactants; white solid; 0.674 g, 90%; mp 203 °C; IR (KBr), 1728, 1653, 1600, 1508 cm^{-1}; ^1H NMR (300 MHz, $CDCl_3$) δ 7.74 (d, $J = 8.8$ Hz, 2H), 7.27 (d, $J = 8.7$ Hz, 2H), 7.16 (d, $J = 8.8$ Hz, 1H), 6.92 (d, $J = 2.3$ Hz, 1H), 6.85–6.74 (m, 5H), 4.15 (t, $J = 5.6$ Hz, 2H), 3.88 (s, 3H) 3.73 (s, 3H), 2.94 (t, $J = 5.6$ Hz, 2H), 2.68 (m, 4H) 1.83 (m, 4H); ^{13}C NMR ($CDCl_3$, 75 MHz) δ 192.6, 163.6, 162.7, 161.2, 159.6, 155.0, 148.4, 131.86, 131.4, 128.4, 127.3, 124.9, 121.5, 114.6, 113.6, 112.8, 111.4, 100.9, 67.0, 55.82, 55.1, 54.6, 54.6, 30.8, 23.4, ESI-MS (*m*/*z*) 499; found 500 $[M + H]^+$; HRMS-ESI: for $C_{30}H_{30}NO_6$ $[M + H]^+$ calcd 500.2073; found 500.2093%.

4.1.3. Representative procedure for the demethylation of compounds 9–11 and 14–19

*Demethylation of compound **9** to 7-hydroxy-4-(4-hydroxy-benzoyl)-3-phenyl-2H-chromen-2-one (compound **20**).* To a mixture of dry dichloromethane (2 ml) and anhydrous aluminum chloride (0.160 g, 1.5 mmol) was added dry ethanethiol (0.5 ml) at 0 °C. The resulting solution was stirred for 10 minutes and 4-(4-hydroxybenzoyl)-7-methoxy-3-phenyl-2*H*-chromen-2-one **9** (0.186 g, 0.5 mmol) was added at 0 °C. The reaction mixture was stirred for 3 h at room temperature. After completion, it was quenched with ice cold water (5 ml) and acidified with 10% aq. HCl (15 ml). The solid precipitate was filtered and purified by column chromatography, eluting with $CHCl_3$–MeOH (25 : 1) to give the title compound; pale yellow solid; yield: 0.170 g, 95%; mp 215 °C; IR (KBr) ν 3481, 3359, 1685, 1596, 1507 cm^{-1}; ^1H NMR (300 MHz, DMSO-d_6) δ 10.65 (brs, 2H), 7.72 (d, $J = 8.7$ Hz, 2H), 7.24–7.20 (m, 5H), 6.98 (d, $J = 8.7$ Hz, 1H), 6.85 (d, $J = 2.2$ Hz, 1H), 6.76–6.71 (m, 3H); ^{13}C NMR (DMSO-d_6, 75 MHz), δ 192.0, 163.9, 161.8, 160.8, 155.3, 149.4, 133.7, 132.7, 130.4, 128.53, 128.2, 127.9, 126.9, 120.6, 116.1, 114.0, 110.1, 102.9; ESI-MS (*m*/*z*): 358 found 359 $[M + H]^+$; HRMS-ES $[M + H]^+$: for $C_{22}H_{15}O_5$ calcd 359.0919; found 359.0878%.

*4-(4-Hydroxybenzoyl)-3-(4-hydroxyphenyl)-2H-chromen-2-one (compound **21**).* Pale yellow solid; yield: 0.165 g, 92%; mp 205 °C; IR (KBr) ν 3310, 1700, 1684, 1575 cm^{-1}; ^1H NMR (300 MHz, DMSO-d_6) δ 10.63 (brs 1H), 9.57 (brs, 1H) 7.74 (d, $J = 8.6$ Hz, 2H), 7.64–7.60 (m, 1H), 7.51 (d, $J = 8.0$ Hz, 1H), 7.29–7.25 (m, 1H), 7.15–7.09 (m, 3H), 6.73 (d, $J = 8.6$ Hz, 2H), 6.62 (d, $J = 8.5$ Hz, 2H); ^{13}C NMR (DMSO-d_6, 75 MHz) δ 192.1, 163.9, 160.6, 158.0, 153.2, 147.6, 132.7, 132.18, 131.7, 126.9, 126.3, 125.2, 125.2, 123.8, 118.1, 117.1, 116.1, 115.0; ESI-MS (*m*/*z*): 358 found 359 $[M + H]^+$; HRMS-ESI: $[M + H]^+$ for $C_{22}H_{15}O_5$ calcd 359.0919, found = 359.0807%.

*7-Hydroxy-4-(4-hydroxybenzoyl)-3-(4-hydroxyphenyl)-2H-chromen-2-one (compound **22**).* Yellow solid; yield: 0.168 g, 90%; mp 240 °C; IR (KBr) ν 3407, 3111, 1663, 1603, 1510, cm^{-1}; ^1H NMR (300 MHz, DMSO-d_6) δ 10.65 (s, 1H), 10.61 (s, IH), 9.50 (s, 1H), 7.69 (d, $J = 8.5$ Hz, 2H), 7.05 (d, $J = 8.4$ Hz 2H), 6.96 (d, $J = 8.7$ Hz, 1H), 6.82 (d, $J = 1.8$ Hz, 1H), 6.74–6.72 (m, 3H), 6.59 (d, $J = 8.4$ Hz, 2H); ^{13}C NMR (DMSO-d_6, 50 MHz) δ 191.8, 163.3, 161.00, 160.5, 157.2, 154.5, 147.9, 132.2, 131.2, 127.19, 126.4, 123.6, 120.2, 115.6, 114.5, 113.4, 109.8; ESI-MS (*m*/*z*): 374 found 375 $[M + H]^+$; HRMS-ESI: $[M + H]^+$ for $C_{22}H_{15}O_6$ calcd 375.0869; found 375.0864%.

*7-Hydroxy-3-phenyl-4-(4-(2-(piperidin-1-yl)ethoxy)benzoyl)-2H-chromen-2-one (compound **23**).* White solid; yield: 0.211 g, 90%; mp 212 °C; IR (KBr) ν 3557, 3165, 1694, 1657, 1598, 1510 cm^{-1}; ^1H NMR (300 MHz, $CDCl_3$ + DMSO-d_6) δ 10.48 (s, 1H), 7.78 (d, $J = 8.6$ Hz, 2H), 7.26–7.21 (m, 5H), 7.007–6.87 (m, 4H), 6.73 (d, $J = 8.6$ Hz, 1H), 4.10 (t, 2H), 2.61 (t, 2H), 2.39 (m, 4H), 1.46–1.36 (m, 6H); ^{13}C NMR (DMSO-d_6, 50 MHz) δ 192.0, 162.4, 161.9, 161.5, 154.8, 148.5, 133.1, 131.9, 129.9, 128.3, 127.7, 127.2, 120.3, 114.9, 113.6, 109.4, 102.6, 62.6, 54.46, 52.5, 22.6, 22.2, 21.1; ESI-MS: (*m*/*z*) 469; found 470 $[M + H]^+$; HRMS-ESI: $[M + H]^+$ for $C_{29}H_{28}NO_5$ 470.1967; found 470.1955%.

*7-Hydroxy-3-phenyl-4-(4-(2-(pyrrolidin-1-yl)ethoxy)benzoyl)-2H-chromen-2-one (compound **24**).* White solid; yield: 0.194 g, 85%; mp 204 °C; IR (KBr) ν 695, 1659, 1597 cm^{-1}; ^1H NMR (300 MHz, DMSO-d_6) δ 10.63 (brs, 1H), 7.62 (d, $J = 8.7$ Hz, 2H), 7.00–6.97 (m, 5H), 6.76–6.65 (m, 4H), 6.53–6.49 (m, 1H), 4.15 (t, 2H), 2.83 (t, 2H), 2.63 (m, 4H) 1.69 (m, 4H); ^{13}C NMR (DMSO-d_6, 75 MHz) δ 192.5, 163.0, 161.9, 160.7, 155.3, 148.9, 133.6, 132.5, 130.4, 128.7, 128.6, 128.2, 127.7, 120.8, 115.4, 114.1, 109.9, 103.1, 64.1, 54.1, 52.8, 23.1; ESI-MS: *m*/*z* 455; found 456 $[M + H]^+$; HRMS-ESI: $[M + H]^+$ for $C_{28}H_{26}NO_5$ $[M + H]^+$ calcd 456.1811 found 456.1806%.

*3-(4-Hydroxyphenyl)-4-(4-(2-(piperidin-1-yl)ethoxy)benzoyl)-2H-chromen-2-one (compound **25**).* Yellow solid; yield: 0.212 g, 90%; mp 224 °C; IR (KBr) ν 3430, 1717, 1663, 1600, 1510 cm^{-1}; ^1H NMR (300 MHz, DMSO-d_6) δ 9.04 (s, 1H),7.64 (d, $J = 7.8$ Hz, 2H), 7.46–7.38 (m, 1H), 7.38–7.31 (m, 1H), 7.14–7.06 (m, 3H), 6.76 (d, $J = 8.0$ Hz, 2H), 6.62 (d, $J = 8.0$ Hz 2H), 4.23 (t, 2H), 2.78 (t, 2H) 2.46 (m, 4H), 1.48–1.44 (m, 6H); ^{13}C NMR (DMSO-d_6, 50 MHz), δ 192.1, 162.5, 160.0, 157.7, 152.7, 146.6, 131.99, 131.2, 128.2, 125.6, 124.9, 123.1, 117.5, 116.7, 114.9, 62.6, 54.4, 52.5, 22.2, 21.1; ESI-MS: (*m*/*z*) 469; found 470 $[M + H]^+$; HRMS-ESI: $[M + H]^+$ for $C_{29}H_{28}NO_5$ calcd 470.1967; found 470.2065%.

*3-(4-Hydroxyphenyl)-4-(4-(2-(pyrrolidin-1-yl)ethoxy)benzoyl)-2H-chromen-2-one (compound **26**).* Yellow solid; yield: 0.201 g, 88%; mp 230 °C; IR (KBr) ν 3498, 1726, 1661, 1598, cm^{-1}; ^1H NMR (300 MHz, DMSO-d_6) δ 11.10 (hump, 1H) 7.65 (d, $J = 8.7$ Hz, 2H), 7.43–7.38 (m, 1H), 7.30 (d, $J = 7.8$ Hz, 1H), 7.07–7.02 (m, 1H), 6.91–6.87 (m, 3H), 6.76 (d, $J = 8.8$ Hz, 2H), 6.43 (d, $J = 8.5$ Hz, 2H), 4.20 (t, 2H), 2.77 (t, 2H) 2.64 (m, 4H), 1.69 (m, 4H); ^{13}C NMR (DMSO-d_6, 50 MHz) δ 192.1, 162.5, 160.89, 157.6, 152.6, 146.6, 132.0, 131.1, 128.1, 124.9, 124.7, 123.1, 117.50, 116.7, 114.9, 63.6, 53.4, 52.2, 22.5; ESI-MS: (*m*/*z*) 455 found 456 $[M + H]^+$, HRMS-ESI: $[M + H]^+$ for $C_{28}H_{26}NO_5$ calcd 456.1811; found 4456.1452%.

*7-Hydroxy-3-(4-hydroxyphenyl)-4-(4-(2-(piperidin-1-yl)ethoxy)-benzoyl)-2H-chromen-2-one (compound **27**).* Yellow solid; yield 0.220 g, 90% mp 256 °C; IR (KBr) ν 3400, 1699, 1657, 1599, cm^{-1}; ^1H NMR (300 MHz, DMSO-d_6) δ 10.49 (brs, 1H), 9.54 (s, 1H), 7.76 (d, $J = 7.8$ Hz, 2H), 6.99 (d, $J = 7.6$ Hz, 2H), 6.91–6.80 (m, 4H), 6.66 (d, $J = 7.5$ Hz, 1H), 6.53 (d, $J = 7.6$ Hz, 2H), 4.11 (t, 2H), 2.63 (t, 2H), 2.40 (m, 4H) 1.46–1.37 (m, 6H); ^{13}C NMR (DMSO-d_6, 50 MHz) δ 192.8, 162.8, 161.6, 160.9, 157.7, 155.1, 147.9, 132.4,

131.7, 128.7, 127.4, 124.0, 120.8, 115.39, 114.0, 110.1, 103.0, 63.1, 53.0, 49.0, 31.1, 22.7, 21.6; ESI-MS: (*m*/*z*) 485 found 486 [M + H]$^+$; HRMS-ESI: [M + H]$^+$ for $C_{29}H_{28}NO_6$ calcd 486.1917; found 486.1942%.

*7-Hydroxy-3-(4-hydroxyphenyl)-4-(4-(2-(pyrrolidin-1-yl)ethoxy)-benzoyl)-2H-chromen-2-one (compound **28**).* Yellow solid; yield: 0.213 g, 90%; mp 248 °C; IR (KBr) ν 3455, 3418, 1704,1663, 1600 cm^{-1}; ^{1}H NMR (300 MHz, $CDCl_3$ + DMSO-d_6) δ 10.18 (brs, 1H), 9.09 (hump, 1H), 7.71 (d, J = 8.2 Hz, 2H), 7.07 (d, J = 8.0 Hz, 2H), 6.98 (d, J = 8.6 Hz, 1H), 6.87–6.85 (m, 3H), 4.11 (t, 2H), 2.76 (t, 2H), 2.38 (m, 4H) 1.66 (m, 4H); ^{13}C NMR (DMSO-d_6, 50 MHz) δ 192.3, 162.4, 161.1, 160.4, 157.2, 154.5, 147.5, 131.9, 131.2, 128.3, 126.9, 123.5, 120.3, 114.9, 114.6, 113.5, 109.6, 102.5, 63.5, 53.5, 52.5, 22.2; ESI-MS: (*m*/*z*) 471 found 472 [M + H]$^+$; HRMS-ESI: [M + H]$^+$ for $C_{28}H_{26}NO_6$ calcd 472.1760; found 472.1799%.

*Synthesis of 4-bromo-7-methoxy-3-phenyl-2H-chromene (compound **31**).* To the solution of isoflavone **30** (5.080 g, 20 mmol) in dry benzene (25 ml), phosphorus tribromide (16.26 g, 60 mmol) was added carefully, and the resulting solution was stirred at 85 °C for 2 h. It was cooled and cautiously poured onto crushed ice (200 g). The aqueous solution was extracted with benzene (50 ml × 3) and the combined organic layers were washed with a saturated aqueous solution of sodium bicarbonate (4 × 40 ml) and brine (2 × 100 ml), dried over Na_2SO_4 and evaporated at reduced pressure. The colourless oil crystallized from methanol at 0 °C on standing for 12 h. The white solid of 4-bromo chromene **31** (5.38 g, 85%) was filtered, dried and used immediately in the next reaction.

*Synthesis of (7-methoxy-3-phenyl-2H-chromen-4-yl)-(4-methoxyphenyl)methanone (compound **34**).* To a stirred solution of **31** (1.59 g, 5 mmol) in dry diethyl ether (15 ml) at 0 °C under nitrogen 1.6 M *n*-butyllithium in hexane (5 ml, 8 mmol) was added slowly *via* syringe in a single portion. The orange solution was stirred at 0 °C for 1.5 h, after which a solution of anisonitrile **32** (0.865 g, 6.5 mmol) in anhydrous ether (10 ml) was added slowly *via* syringe in a single portion. The solution was stirred for 1.5 h at 10 °C. After completion of the reaction the reaction mixture was poured into water and extracted with ethyl acetate (30 ml × 4), dried over Na_2SO_4 and concentrated at reduced pressure to give a brown semisolid, which was purified through column chromatography with hexane ethylacetate (10 : 1); yellow solid; yield: 1.39 g, 75% mp 130 °C; IR (KBr) 1620, 1534 cm^{-1}; ^{1}H NMR (300 MHz, $CDCl_3$) δ 7.80 (d, J = 8.7 Hz, 2H), 7.22–7.19 (m, 5H),6.87–6.83 (m, 3H) 6.5 (d, J = 2.4 Hz, 1H), 6.39 (dd, J = 8.5 Hz, J = 2.43 Hz, 1H), 5.11 (s, 2H), 3.81 (s, 3H), 3.79 (s, 3H); ^{13}C NMR (75 MHz, $CDCl_3$) 174.2, 161.9, 160.9, 154.6, 136.8, 132.5, 130.1, 129.6, 128.4, 127.7, 127.2, 126.9, 126.8, 115.5, 113.8, 107.6, 101.9, 69.20, 55.4, 55.3.0; ESI-MS: (*m*/*z*) 372; found 372[M]$^+$; HRMS-ESI: [M]$^+$ for $C_{24}H_{20}O4$ 372.1362 found 372.1641%.

*(4-(2-Chloroethoxy)phenyl)(7-methoxy-3-phenyl-2H-chromen-4-yl)methanone (compound **35**).* Compound **35** was synthesized from compound **31** and nitrile **33**. Yellow solid; yield: 1.470 g, 70%; mp 135 °C; IR, (KBr), ν 1640, 1544 cm^{-1}; ^{1}H NMR (300 MHz, $CDCl_3$) δ 7.81 (d, J = 8.46 Hz, 2H), 7.22 (m, 5H), 6.86–6.84 (m, 3H) 6.53 (d, J = 2.46 Hz, 1H), 6.39 (dd, J = 8.55 Hz, J = 2.46 Hz, 1H), 5.10 (s, 2H), 4.23 (t, J = 5.82 Hz, 2H), 3.83–3.81 (t, J = 5.79, 2H), 3.79 (s, 3H); ^{13}C NMR (75 MHz, $CDCl_3$) δ 174.1, 160.9, 160.4, 154.6, 136.7, 132.3, 130.7, 129.7, 128.4, 127.8, 127.2, 126.7, 115.4, 114.4, 107.6, 101.9, 69.1, 67.9, 55.4, 41.7; ESI-MS: (*m*/*z*) 420; found 420 [M]$^+$.

*(4-(2-Chloroethoxy)phenyl)(7-hydroxy-3-phenyl-2H-chromen-4-yl)methanone (compound **38**).* Compound **38** was synthesized from compound **35** (1.260 g, 3 mmol) according to the procedure of demethylation used for the synthesis of compound **20**. Solid residue after vacuum drying was purified by chromatography on a silica gel column (chloroform–methanol, 50 : 1) to give a pale yellow solid; yield: 0.820 g, 70%; mp 142 °C; IR KBr ν 3318, 1721, 1605, 1503 cm^{-1}; ^{1}H NMR (300 MHz, DMSO-d_6) δ 10.30 (brs, 1H), 7.70 (d, J = 7.6 Hz, 2H), 7.29–7.19 (m, 5H), 6.92 (d, J = 8.8 Hz, 2H), 6.57 (d, J = 7.1 Hz, 1H), 6.34 (d, J = 2.2 Hz, 1H), 6.27 (m, 1H) 5.05 (s, 2H), 4.24 (t, J = 4.6 Hz, 2H), 3.92 (t, J = 5.16 Hz, 2H); ^{13}C NMR (50 MHz, DMSO-d_6) δ 171.4, 159.9, 158.8, 154.2, 136.9, 131.5, 130.24, 129.0, 128.1, 127.4, 126.8, 114.3, 113.8, 108.8, 102.8, 68.3, 67.9, 42.8; ESI-MS: (*m*/*z*) 390; found 390 [M]$^+$.

4.1.4. General procedure for the synthesis of compound 36–37 and 39–40

*(7-Methoxy-3-phenyl-2H-chromen-4-yl)(4-(2-(piperidin-1-yl)-ethoxy)phenyl)methanone (compound **36**).* To a stirred solution of compound **35** (0.420 g, 1 mmol) in dry DMF (10 ml) was added TBAI (6 mg) and piperidine (0.3 ml) and the resulting solution was stirred at 80 °C for 6 h. After completion of the reaction, the reaction mixture was poured into ice water, the solid precipitate was filtered and after vacuum drying it was crystallized from hexane to afford the title compound as a white solid; yield: 0.445 g, 95%; mp 156 °C. IR (KBr) ν 1730, 1615, 1503, cm^{-1}. ^{1}H NMR (300 MHz, $CDCl_3$) δ 7.78 (d, J = 8.3 Hz, 2H), 7.22–7.20 (m, 5H), 6.87–6.82 (m, 3H) 6.53 (d, J = 2.4 Hz, 1H), 6.38 (dd, J = 8.5 Hz, J = 2.4 Hz, 1H), 5.10 (s, 2H), 4.10 (t, J = 6.1 Hz), 3.79 (s, 3H), 2.76 (t, J = 6.0 Hz, 2H), 2.50 (t, J = 4.59, Hz 4H), 1.46–1.45 (m, 6H); ^{13}C NMR (75 MHz, $CDCl_3$) δ 174.2, 161.1, 160.9, 154.6, 136.8, 132.5, 130.1, 129.5, 127.7, 127.19, 126.9, 115.5, 114.4, 107.6, 101.8, 69.2, 65.9, 57.7, 55.38, 55.0, 25.8, 24.1; ESI-MS: (*m*/*z*) 469; found 469 [M]$^+$; HRMS-ESI: [M]$^+$ for $C_{30}H_{31}NO_4$ calcd 469.2253; found 469.2477%.

*(7-Methoxy-3-phenyl-2H-chromen-4-yl)(4-(2-(pyrrolidin-1-yl)-ethoxy) phenyl)methanone (compound **37**).* White solid; yield: 0.409 g, 90%; mp 152 °C; IR (KBr), ν 3142, 2918, 2872, 2271, 1722, 1605, 1503, 1461, 1362, 1254, 1159, 1023, 850, 761 cm^{-1}; ^{1}H NMR (300 MHz, $CDCl_3$) δ 7.78 (d, J = 7.2 Hz, 2H), 7.21–7.19 (m, 5H), 6.86–6.84 (m, 3H) 6.53 (d, J = 2.4 Hz, 1H), 6.38 (dd, J = 8.7 Hz, J = 2.6 Hz, 1H), 5.10 (s, 2H), 4.11 (t, J = 6.0 Hz, 2H), 3.79 (s, 3H), 2.90 (t, J = 5.9 Hz, 2H), 2.62 (m, 4H), 1.86–1.81 (m, 4H); ^{13}C NMR (75 MHz, $CDCl_3$) δ 174.26, 161.19, 160.95, 154.61, 136.84, 130.11, 129.56, 128.42, 127.76, 127.19, 126.81, 115.52, 114.38, 107.65, 101.88, 69.20, 67.10, 55.39, 54.94, 54.71, 23.49; ESI-MS: (*m*/*z*) 455; found 455 [M]$^+$; HRMS-ESI: [M]$^+$ for $C_{29}H_{29}NO_4$ calcd 455.2097; found 455.2322%.

*(7-Hydroxy-3-phenyl-2H-chromen-4-yl)(4-(2-(piperidin-1-yl)-ethoxy)phenyl)methanone (compound **39**).* White solid; yield: 0.432 g, 95%; mp 168 °C. IR (KBr), ν 3442, 2934, 1718, 1605, cm^{-1}. ^{1}H NMR (300 MHz, $CDCl_3$ + CD_3OD) δ 7.75 (d, J = 8.5 Hz, 2H), 7.19 (m, 5H), 6.7–6.69 (m, 3H), 6.41 (d, J = 2.1 Hz, 1H), 6.22

(dd, $J = 8.3$ Hz, $J = 2.1$ Hz, 1H), 5.01 (s, 2H), 4.11 (t, $J = 5.6$ Hz, 2H), 2.80 (t, $J = 5.4$ Hz, 2H), 2.57 (m, 4H), 1.65–1.63 (m, 4H), 1.48–1.39 (m, 2H); ^{13}C NMR (75 MHz, $CDCl_3$) δ 174.2, 164.4, 161.9, 157.8, 140.1, 135.5, 133.0, 131.67.4, 130.4, 130.2, 130.0, 117.7, 112.4, 106.5, 72.3, 68.5, 60.8, 58.0, 28.5, 27.1; ESI-MS: (m/z) 455; found 455 $[M]^+$, HRMS-ESI: $[M]^+$ for $C_{29}H_{29}NO_4$ calcd 455.2097; found 455.2036%.

*(7-Hydroxy-3-phenyl-2H-chromen-4-yl)(4-(2-(pyrrolidin-1-yl)-ethoxy)phenyl)methanone (compound **40**).* White solid; yield: 0.397 g, 90%; mp 160 °C; IR (KBr), ν 3552, 1722, 1596 cm^{-1}; ^{1}H NMR (300 MHz, $CDCl_3$) δ 7.75 (d, $J = 8.6$ Hz, 2H), 7.19 (m, 5H), 6.77 (d, $J = 8.7$ Hz, 2H) 6.68 (d, $J = 8.4$ Hz, 1H), 6.39 (d, 2.6 Hz, 1H), 6.19 (dd, $J = 8.3$ Hz, $J = 2.0$ Hz, 1H), 5.05 (s, 2H), 4.11 (t, $J =$ 5.4 Hz, 2H), 2.96 (t, $J = 5.5$ Hz, 2H), 2.78–2.71 (m, 4H), 1.85 (m, 4H); ^{13}C NMR (75 MHz, $CDCl_3$) δ 175.4, 161.2, 158.88, 154.7, 137.0, 131.9, 129.5, 128.0, 127.4, 127.2, 127.1, 126.4, 114.3, 114.2, 108.7, 102.9, 68.8, 66.2, 54.4, 54.2, 22.9; ESI-MS (m/z): 441 found 441 $[M]^+$; HRMS-ESI: $[M]^+$ for $C_{28}H_{27}NO_4$ calcd 441.1940; found 441.2179%.

4.1.5. General procedure for the synthesis of compound 43–46

*(7-Methoxy-2,2-dimethyl-3-phenyl-2H-chromen-6-yl)(4-methoxyphenyl)methanone (compound **43**).* To the ice cooled stirred solution of 7-methoxy-2,2-dimethyl-isoflavene **42** (0.532 g, 2 mmol), and anisoyl chloride (0.341 g, 2 mmol) in dry dichloromethane (10 ml) was added $SnCl_4$ (0.782 g, 3 mmol) slowly. The reaction mixture was stirred with cooling until the starting material was consumed and then cold 2N HCl (10 ml) was added to the reaction mixture. The organic phase was separated and the aqueous phase was further extracted once with dichloromethane (15 ml). The collected organic layers were washed with water (20 ml × 2) and finally with brine (20 ml × 3). The combined organic layer was dried over Na_2SO_4. After filtration and evaporation, the solid was crystallized from hexane to afford the pure product. White solid; yield: 0.760 g, 95%; mp 126 °C; IR (KBr), ν 1670, 1607, 1496 cm^{-1}; ^{1}H NMR (300 MHz, $CDCl_3$) δ 7.82 (d, $J = 8.8$ Hz, 2H), 7.35–7.30 (m, 5H), 7.12 (s, 1H) 6.91 (d, $J = 8.8$ Hz, 2H), 6.52 (s, 1H), 6.28 (s, 1H), 3.87 (s, 3H), 3.73 (s, 3H), 1.58 (s, 6H); ^{13}C NMR (75 MHz, $CDCl_3$) δ 194.5, 163.5, 159.2, 156.2, 140.0, 139.5, 132.4, 131.5, 128.5, 128.4, 128.3, 127.7, 122.3, 121.5, 115.6, 113.5, 100.2, 80.0, 55.9, 55.6, 29.9, 27.4; ESI-MS: (m/z) 400, found; 401 $[M + H]^+$ HRMS-ESI calcd for $C_{26}H_{25}O_4$ $[M + H]^+ = 401.1753$ found 401.1747%.

*(4-(2-Chloroethoxy)phenyl)(7-methoxy-2,2-dimethyl-3-phenyl-2H-chromen-6yl)methanone (compound **44**).* White solid; yield: 0.852 g, 95%; mp 128 °C; IR (KBr), ν 1680, 1630, 1512 cm^{-1}; ^{1}H NMR (300 MHz, $CDCl_3$) δ 7.83 (d, $J = 8.8$ Hz, 2H), 7.35–7.31 (m, 5H), 7.14 (s, 1H) 6.94 (d, $J = 8.8$ Hz, 2H), 6.53 (s, 1H), 6.29 (s, 1H), 4.31 (t, $J = 5.8$ Hz, 2H), 3.86 (t, $J = 5.8$ Hz, 2H), 3.87 (s, 3H), 3.74 (s, 3H), 1.59 (s, 6H); ^{13}C NMR (75 MHz, $CDCl_3$) δ 194.5, 163.5, 159.2, 156.2, 140.0, 139.5, 132.4, 131.5, 128.5, 128.4, 128.3, 127.7, 122.3, 121.5, 115.6, 113.5, 100.2, 80.0, 55.9, 55.6, 29.9, 27.4; ESI-MS: (m/z) 448; found 449; $[M + H]^+$.

*(7-Methoxy-2,2-dimethyl-3-phenyl-2H-chromen-6-yl)(4-(2-(piperidin-1-yl)ethoxy)phenyl) methanone (compound **45**).* Compound **45** was prepared from compound **44** (0.448 g, 1 mmol), according to the procedure which was used for the synthesis of compound **36**. White solid; yield: 0.473 g, 95%; mp 132 °C; IR (KBr), ν 1643, 1604, 1495 cm^{-1}; ^{1}H NMR (300 MHz, $CDCl_3$) δ 7.81 (d, $J = 8.7$ Hz, 2H), 7.35–7.33 (m, 5H), 7.12 (s, 1H), 6.92 (d, $J = 8.7$ Hz, 2H), 6.52 (s, 1H), 6.29 (s, 1H), 4.18 (t, $J = 5.9$ Hz, 2H), 3.78 (s, 3H), 2.80 (t, $J = 5.9$ Hz, 2H), 2.53 (m, 4H), 1.64–1.58 (m, 12H); ^{13}C NMR (50 MHz, $CDCl_3$) δ 194.2, 162.5, 158.9, 156.0, 139.8, 139.2, 132.2, 131.3, 128.2, 127.4, 122.0, 121.3, 115.4, 113.8, 100.0, 9.80, 66.1, 55.7, 55.50, 55.0, 27.2, 25.8, 24.1; ESI-MS: (m/z) 497; found 498 $[M + H]^+$; HRMS-ESI: $[M + H]^+$ for $C_{32}H_{36}NO_4$ calcd 498.2644; found 498.2648%.

*(7-Methoxy-2,2-dimethyl-3-phenyl-2H-chromen-6-yl)(4-(2-(pyrrolidin-1-yl) ethoxy)phenyl)methanone (compound **46**).* Compound **46** was prepared from compound **44** according to the procedure used for the synthesis of compound **36**. White solid; 0.445 g, 92%; mp 125 °C; IR (KBr), ν 1642, 1601, 1494 cm^{-1}; ^{1}H NMR (300 MHz, $CDCl_3$) δ 7.81 (d, $J = 8.5$ Hz, 2H), 7.35–7.33 (m, 5H), 7.13 (s, 1H) 6.94 (d, $J = 8.6$ Hz, 2H), 6.52 (s, 1H), 6.29 (s, 1H), 4.19 (t, $J = 5.8$ Hz, 2H), 3.74 (s, 3H), 2.94 (t, $J = 5.7$ Hz, 2H), 2.65 (m, 4H), 1.83 (m, 4H), 1.59 (s, 6H) ^{13}C NMR (50 MHz, $CDCl_3$) δ 194.2, 162.5, 158.9, 155.9, 139.8, 139.2, 132.1, 131.4, 128.2, 127.4, 122.0, 121.3, 115.4, 113.8, 100.0, 79.7, 67.2, 55.7, 55.7, 54.8, 54.7, 27.2, 23.4; ESI-MS: (m/z) 483; found 484 $[M + H]^+$; HRMS-ESI: $[M + H]^+$ for $C_{31}H_{34}NO_4$ calcd 484.2488; found 484.2485%.

4.2. Materials and methods

4.2.1. Cell culture. Human breast cancer cell lines MCF-7, MDA-MB231 and normal human kidney cell line, HEK293, were purchased from American Type Culture Collection (Manassas, VA, USA). Human endometrial cancer cell line Ishikawa was purchased from European Collection of Cell Cultures. They were maintained in DMEM supplemented with 10% fetal bovine serum (FBS). Cells were cultured at 37 °C and 5% CO_2. Prior to the experiments, cells were cultured in phenol red-free DMEM supplemented with 10% charcoal stripped fetal bovine serum.

4.2.2. Cell proliferation assay (MTT assay) in cancer cell lines and normal cell line. The antiproliferative activities of the compounds in various cell lines were determined using MTT (3-(4,5-dimethylthiazol-2-yl)-2,5-diphenyl tetrazolium bromide) reduction assay.[39] 2.5×10^3 cells per well were seeded in 100 μl DMEM (Dulbecco's Modified Eagle's Medium) supplemented with 10% FBS in each well of 96-well microculture plates and incubated for 24 h at 37 °C in a CO_2 incubator. The compounds were diluted to the desired concentration in the culture medium. After 48 h of incubation, the media were removed and 100 μl MTT (0.5 mg ml^{-1}) was added to each well and the plates were further incubated for 3 h. Supernatant from each well was carefully removed, formazan crystals were dissolved in 100 μl DMSO, and absorbance at a wavelength of 540 nm was recorded.

4.2.3. Transient transfection and transactivation assay. Once the cells attained 80–90% confluence, COS-1 cells were transfected with 50 ng of expression vector for ERα (pSG5 ERα) or 50 ng of expression vector for hERβ (pSG5–ERβ) along with 100 μg of luciferase reporter gene construct pGL3 2 × ERE pS2 Luc (plasmids were generous gifts from Prof. M. G. Parker,

Imperial Cancer Research Fund, London, UK), using Lipofectamine-2000™ transfection reagent (Invitrogen) as per the manufacturer's protocol. To normalize for transfection efficiencies, pRL-SV40-*luc* (Promega) was used. After transfection, cells were trypsinized and seeded (2×10^4 cells per well) into a 96-well plate. The cells were incubated with E_2 (10 nM) and various compounds (1 μM, 10 μM and 20 μM) for 24 h. For antagonistic activity, E_2 was included in the incubation with compounds. Luciferase activity was measured using Dual Luciferase Assay System (Promega) according to the manufacturer's protocol to detect the ER–ERE-mediated transcriptional activity. The firefly luciferase intensity for each sample was normalized based on transfection efficiency measured by renilla luciferase activity.[40]

4.2.4. Transient SiRNA transfection. MCF-7 cells were transiently transfected with SiRNA (20 nM) specific for either ERα or ERβ or the negative control (random sequence without any homology with mammalian gene) (Invitrogen) using lipofectamine rnaimax reagent (Invitrogen). Transfection was performed in a 96-well plate using the reverse transfection method as per the manufacturer's instructions. After 18 h of transfection, cells were treated with compounds at IC_{50} values for 48 h and cell viability was assessed using MTT assay as described.[41] PPT and DPN were used as ERα and ERβ agonists, respectively. E_2 was used as reference estrogen.

4.2.5. Alkaline phosphatase (ALP) assay. Estrogenic stimulation was measured in Ishikawa human endometrial cancer cells by ALP quantitation (**20**, **21**). The cells were incubated in MEM/F-12, supplemented with 5% DCC-stripped fetal bovine serum, L-glutamine (2 mM), MEM sodium pyruvate (1 mM), and HEPES (2 mM). For the agonist mode, plates received diluted compounds. Cells were incubated for 24 hours, and then fresh compounds were added for an additional 48 hours. The assay was quenched by removing the medium and rinsing the plates twice in phosphate-buffered saline, and the plates were dried for 5 minutes and frozen at −70 °C for at least 30 minutes. After thawing, 100 ml *p*-nitrophenyl phosphate (PNPP) was added over 20 minutes at 37 °C, and the plates were read on a spectrophotometer at 405 nm. For the agonist mode, a percentage increase over control was calculated. The ALP activity was calculated as a percentage of activity of the control group.

4.3. Anti-osteoporotic activity

Cell culture media and supplements were purchased from Invitrogen (Carlsbad, CA). All fine chemicals were purchased from Sigma-Aldrich (St. Louis, MO). HPLC grade acetonitrile was obtained from Merck India Ltd (Mumbai, India).

4.3.1. Alkaline phosphatase activity. For the measurement of alkaline phosphatase (ALP) enzyme activity, RCOs at approximately 80% confluence were trypsinized, and 2×10^3 cells were seeded onto 96-well plates. Cells were treated with compounds with different concentrations (100 μM, 1.0 μM, 10 nM, 100 pM, 1.0 pM) or vehicle for 48 hours in a α-MEM supplemented with 10% FBS, 10 mM β-glycerophosphate, 50 μg ml^{-1} ascorbic acid, and 1% penicillin/streptomycin (osteoblast differentiation medium). At the end of the incubation period, total ALP activity was measured using *p*-nitrophenylphosphate (PNPP) as the substrate, and absorbance was read at 405 nm.[42]

4.3.2. Culture of rat calvarial osteoblasts (RCOs). Rat calvarial osteoblasts were obtained following our previously published protocol of sequential digestion.[43] Briefly, 8–10 calvaria from 1 to 2-day-old S.D. rat (both sexes) were isolated. After surgical isolation from the skull and the removal of sutures and adherent mesenchymal tissues, calvaria were subjected to five sequential (10–15 min) digestions at 37 °C in a solution containing 0.1% dispase and 0.1% collagenase P. Cells released from the second to fifth digestions were collected, centrifuged, resuspended, and plated in T-25 cm^2 flasks in α-MEM containing 10% FCS and 1% penicillin/streptomycin (complete growth medium).

4.3.3. Mineralization of calvarial osteoblasts. Calvarial osteoblasts cultured until 80% confluence were trypsinized and plated in the differentiation medium (2.5×10^4 cells per well in a 12-well plate), consisting of complete growth medium with ascorbic acid (50 μg ml^{-1}) and β-glycerophosphate (10 mM). The medium was changed every alternate day up to 21 days. A 10 mM stock solution of the compound was made in DMSO. The treatment group contained the osteoblast differentiation medium at different concentrations (10 nM, 100 pM) of compounds. At the end of the experiment, cells were washed with PBS and fixed with 4% paraformaldehyde in PBS for 15 min. The fixed cells were stained with 40 mM (pH 4.5) alizarin red-S for 30 min followed by washing with water.[44] For quantification of staining, 800 μl of 10% (v/v) acetic acid was added to each well, and the plates were incubated at room temperature for 30 min with shaking. The monolayer, now loosely attached to the plate, was then scraped from the plate with a cell scraper and transferred in 10% (v/v) acetic acid to a 1.5 ml tube. After vortexing for 30 s, the slurry was overlaid with 500 μl mineral oil (Sigma-Aldrich), heated to exactly 85 °C for 10 min, and transferred to ice for 5 min. The slurry was then centrifuged at 20000*g* for 15 min and 500 μl of the supernatant was removed to a new tube. Then 200 μl of 10% (v/v) ammonium hydroxide was added to neutralize the acid. In some cases, the pH was measured at this point to ensure that it was between 4.1 and 4.5. OD (405 nm) of 150 μl aliquots of the supernatant were measured in 96-well format using opaque-walled, transparent-bottomed plates.[45]

Acknowledgements

The authors (M. K. H., M. I. A., N. Y., P. K. G., R. S., M. M., P. K.) are thankful for financial assistance in the form of SRF by CSIR, New Delhi, India, (I. F.,V. K., J. G.) UGC India, A. K. G ICMR, New Delhi and PRM thanks to CSIR, New Delhi, for the Grant-in-aid of Emeritus Scientist, Scheme [no. 21(0766)/09/EMR-II]. Furthermore, all are grateful to the Sophisticated Analytical Instrument Facility (SAIF) CDRI, Lucknow, India, for providing spectral analysis/data of pure compounds and the Ministry of Health and Family Welfare for financial assistance. CDRI communication no. 8568.

Notes and references

1 A. Jemal, F. Bray, M. Melissa, J. Ferlay, E. Ward and D. Forman, Global Cancer statistics, *Ca-Cancer J. Clin.*, 2011, **61**, 69.

2 American Cancer Society, *Cancer Facts & Figures*, 2012, http://www.cancer.org/acs/groups/content/@epidemiologysurveilance/documents/document/acspc-031941.pdf.

3 B. S. Katzenellenbogen, *Biol. Reprod.*, 1996, **54**, 287.

4 P. S. Danielian, R. White, J. A. Lees and M. G. Parker, *EMBO J.*, 1992, **11**, 1025.

5 P. Huang, V. Chandra and F. Rastinejad, *Annu. Rev. Physiol.*, 2010, **72**, 247.

6 J. S. Lewis and V. C. Jordan, *Mutat. Res.*, 2005, **591**, 247.

7 G. G. Kuiper, B. Carlsson, K. Grandien, E. Enmark, J. Haggblad, S. Nilsson and J. Å. Gustafsson, *Endocrinology*, 1997, **138**, 863.

8 S. Nilsson and J. Å. Gustafsson, *Clin. Pharmacol. Ther.*, 2011, **89**, 44.

9 C. Thomas and J. Å. Gustafsson, *Nat. Rev. Cancer*, 2011, **11**, 597.

10 V. Speirs, G. P. Skliris, S. E. Burdall and P. J. Carder, *J. Clin. Pathol.*, 2002, **55**, 371.

11 E. S. Manas, Z. B. Xu, R. J. Unwalla and W. S. Somers, *Structure*, 2004, **12**, 2197–2207.

12 J. A. Katzenellenbogen, *J. Med. Chem.*, 2011, **54**, 5271.

13 S. Nilsson, K. F. Koehler and J. Å. Gustafsson, *Nat. Rev. Drug Discovery*, 2011, **10**, 778.

14 S. Ali, L. Buluwela and R. C. Coombes, *Annu. Rev. Med.*, 2011, **62**, 217.

15 (*a*) V. C. Jordan, *J. Med. Chem.*, 2003, **46**, 883; (*b*) V. C. Jordan, *J. Med. Chem.*, 2003, **46**, 1081.

16 (*a*) I. Kostova, *Curr. Med. Chem.: Anti-Cancer Agents*, 2005, **5**, 29; (*b*) D. Egan, E. O'Kennedy, E. Moran, D. Cox, E. Prosser and R. D. Thornes, *Drug Metab. Rev.*, 1990, **22**, 503.

17 M. A. Musa, J. S. Cooperwood and M. O. F. Khan, *Curr. Med. Chem.*, 2008, **15**, 2664.

18 J. R. S. Hoult and M. Paya, *Gen. Pharmacol.*, 1996, **27**, 713.

19 L. W. L. Woo1, A. Purohit, B. Malini, M. J. Reed and B. V. L. Potter, *Chem. Biol.*, 2000, **7**, 773.

20 H. Brady, M. Doubleday, L. M. Gayo-Fung, M. Hickman, S. Khammungkhune, A. Kois, S. Lipps, S. Pierce, N. Richard, G. Shevlin, M. K. Sutherland, D. W. Anderson, S. Bhagwat and B. Stein, *Mol. Pharmacol.*, 2002, **61**, 562.

21 N. S. I. Wind and I. Holen, *Int. J. Breast Cancer*, 2011, **2011**, 967419.

22 J. Liang and Y. Shang, *Annu. Rev. Physiol.*, 2013, **75**, 225.

23 D. Yue, T. T. Tuanli and R. C. Larock, *J. Org. Chem.*, 2005, **70**, 10292.

24 C. Mousset, O. Provot, A. Hamze, J. Bignon, J. D. Brion and M. Alami, *Tetrahedron*, 2008, **64**, 4287.

25 (*a*) J. A. Dodge, M. G. Stocksdale, K. J. Fahey and C. D. Jones, *J. Org. Chem.*, 1995, **60**, 739; (*b*) C. J. Lion, D. A. Vasselin, C. H. Schwalbe, C. S. Matthews, M. F. G. Stevensa and A. D. Westwell, *Org. Biomol. Chem.*, 2005, **3**, 3996.

26 (*a*) K. Wähälä and A. Hase, *J. Chem. Soc., Perkin Trans. 1*, 1991, 3005–3008; (*b*) S. Balasubramanian and M. G. Nair, *Synth. Commun.*, 2000, **30**, 469.

27 K. S. Singh, V. Saibaba, V. Ravikumar, V. Santosh, Rudrawar, P. Daga, C. S. Rao, V. Akhila, P. Hegde and K. Rao, *Bioorg. Med. Chem. Lett.*, 2004, **12**, 1881.

28 R. Gandhidasan, S. Neelkantan and P. V. Raman, *Synthesis*, 1982, 1110.

29 S. D. Prasad, (A2) WO 2009078029, 2009.

30 A. M. Brzozowski, A. C. W. Pike, Z. Dauter, R. E. Hubbard, T. Bonn, L. E. O. Ohman, G. L. Greene, J.-Å. Gustafsson and M. Carlquist, *Nature*, 1997, **389**, 753.

31 A. C. W. Pike, A. M. Brzozowski, R. E. Hubbard, T. Bonn, A. G. Thorsell, J. E. O. Ljunggren, J. Å. Gustaffson and M. Carlquist, *EMBO J.*, 1999, **17**, 4608.

32 *Schrödinger, version 9.1*, Schrödinger, LLC, New York, 2005.

33 B. S. Katzenellenbogen, *Biol. Reprod.*, 1996, **54**, 287.

34 P. S. Danielian, R. White, J. A. Lees and M. G. Parker, *EMBO J.*, 1992, **11**, 1025.

35 M. Beato and A. Sanchez-Pacheco, *Endocr. Rev.*, 1996, **17**, 587.

36 E. A. Ariazi, J. L. Ariazi, F. Cordera and V. C. Jordan, *Curr. Top. Med. Chem.*, 2006, **6**, 181.

37 J. L. Plouffe and C. M. Facoq, *J. Soc. Gynecol. Invest.*, 2000, **7**, S38–S46.

38 *GOLD, Version 3.1*, Cambridge Crystallographic Data Centre, Cambridge, UK.

39 I. Fatima, V. Chandra, R. Saxena, M. Manohar, Y. Sanghani, K. Hajela, M. P. S. Negi, P. L. Sankhwar, S. K. Jain and A. Dwivedi, *Mol. Cell. Endocrinol.*, 2012, **348**, 198.

40 C. S. Blesson, S. Awasthi, G. Kharkwal, A. Daverey and A. Dwivedi, *Steroids*, 2006, **71**, 993.

41 R. Saxena, I. Fatima, V. Chandra, C. S. Blesson, G. Kharkwal, M. K. Hussain, K. Hajela, B. G. Roy and A. Dwivedi, *Steroids*, 2013, **78**, 1071.

42 K. V. Sashidhara, M. Kumar, V. Khedgikar, P. Kushwaha, R. K. Modukuri, A. Kumar, J. Gautam, D. Singh, B. Sridhar and R. Trivedi, *J. Med. Chem.*, 2013, **56**, 109.

43 G. L. Wong and D. V. Cohn, *Proc. Natl. Acad. Sci. U. S. A.*, 1975, **72**, 3167.

44 J. A. Siddiqui, G. Swarnkara, K. Sharana, B. Chakravartia, G. Sharmaa, P. Rawatb, M. Kumarb, F. M. Khan, D. Pierrozc, R. Maurya and N. Chattopadhyaya, *Mol. Cell. Endocrinol.*, 2010, **323**, 256.

45 (*a*) C. A. Gregory, W. G. Gunn, A. Peister and D. J. Prockop, *Anal. Biochem.*, 2004, **329**, 77; (*b*) J. Gautam, P. Kushwaha, G. Swarnkar, V. Khedgikar, G. K. Nagar, D. Singh, V. Singh, M. Jain, M. Barthwal and R. Trivedi, *Phytomedicine*, 2012, **19**, 1134; (*c*) V. Khedgikar, J. Gautam, P. Kushwaha, A. Kumar, G. K. Nagar, P. Dixit, R. Chillara, Voruganti, S. Singh, Wahajuddin, R. Maurya, N. Chattopadhyay and R. Trivedi, *Menopause*, 2012, **19**, 1336.